APPROVED FOR RELEASE: 2007/02/08: CIA-RDP82-00850R000300010007-0

APPROVED FOR RELEASE: 2007/02/08: CIA-RDP82-00850R000300010007-0

APPROVED FOR RELEASE: 2007/02/08: CIA-RDP82-00850R000300010007-0

JPRS L/9224

28 July 1980

USSR Report

EARTH SCIENCES

(FOUO 6/80)

FBIS FOREIGN BROADCAST INFORMATION SERVICE

APPROVED FOR RELEASE: 2007/02/08: CIA-RDP82-00850R000300010007-0

APPROVED FOR RELEASE: 2007/02/08: CIA-RDP82-00850R000300010007-0

NOTE

JPRS publications contain information primarily from foreign newspapers, periodicals and books, but also from news agency transmissions and broadcasts. Materials from foreign-language sources are translated; those from English-language sources are transcribed or reprinted, with the original phrasing and other characteristics retained.

Headlines, editorial reports, and material enclosed in brackets [] are supplied by JPRS. Processing indicators such as [Text] or [Excerpt] in the first line of each item, or following the last line of a brief, indicate how the original information was processed. Where no processing indicator is given, the information was summarized or extracted.

Unfamiliar names rendered phonetically or transliterated are enclosed in parentheses. Words or names preceded by a question mark and enclosed in parentheses were not clear in the original but have been supplied as appropriate in context. Other unattributed parenthetical notes within the body of an item originate with the source. Times within items are as given by source.

The contents of this publication in no way represent the policies, views or attitudes of the U.S. Government.

For further information on report content call (703) 351-2938 (economic); 3468 (political, sociological, military); 2726 (life sciences); 2725 (physical sciences).

COPYRIGHT LAWS AND REGULATIONS GOVERNING OWNERSHIP OF MATERIALS REPRODUCED HEREIN REQUIRE THAT DISSEMINATION OF THIS PUBLICATION BE RESTRICTED FOR OFFICIAL USE ONLY.

APPROVED FOR RELEASE: 2007/02/08: CIA-RDP82-00850R000300010007-0

APPROVED FOR RELEASE: 2007/02/08: CIA-RDP82-00850R000300010007-0

JPRS L/9224

28 July 1980

USSR REPORT

EARTH SCIENCES

(FOUO 6/80)

CONTENTS

APPROVED FOR RELEASE: 2007/02/08: CIA-RDP82-00850R000300010007-0

APPROVED FOR RELEASE: 2007/02/08: CIA-RDP82-00850R000300010007-0

OCEANOGRAPHY

UDC 551.465.41

STRUCTURE OF THE MIXED LAYER IN A STRATIFIED FLUID

Moscow IZVESTIYA AKADEMII NAUK SSSR, FIZIKA ATMOSFERY I OKEANA in Russian
Vol 16, No 3, 1980 pp 284-293

[Article by V. A. Popov and Yu. D. Chashechkin, All-Union Scientific Research Institute of Physical-Technical and Radio Engineering Measurements, submitted for publication 22 February 1979, resubmitted after revisions 4 May 1979]

Abstract: Optical and contact methods were used for investigating the structure of the mixed layer in a stably stratified fluid arising under the influence of a constant velocity shear at the free surface. In the case of small shearing stresses, when the global Richardson number $Ri_0 > 0.3$, a two-layer circulation current is formed with a sloping interface between the layers whose total thickness remains virtually constant with time. In the case of great velocity shearing stresses, when $Ri_0 < 0.1$, the thickness of the turbulent mixed layer increases with time as $t^{0.25}$.

[Text] Interest in investigation of the dynamics of formation of mixed layers in a stratified fluid under the influence of turbulence excited by external sources is caused for the most part by the study of the mechanisms of formation of the upper mixed layer, the seasonal thermocline and the thin stratified structure of the ocean [1]. In addition to the extremely complex and time-consuming field investigations, extensive use has been made of laboratory modeling methods, making it possible to carry out experiments under controllable and reproducible conditions.

A turbulent disturbance, mixing the fluid in one of the layers, under laboratory conditions is created by an oscillating grid [2], constant shearing stress at the surface of the fluid [3], ejection and sampling of the fluid from the layer [4]. In a fluid with a vertical density gradient ($\rho = \rho_0(z)$, $\Lambda = (d \ln \rho/dz)^{-1}$ is the density scale, $N(z) = (g\Lambda^{-1})^{1/2}$ is the frequency of free internal oscillations) there is formation

APPROVED FOR RELEASE: 2007/02/08: CIA-RDP82-00850R000300010007-0

APPROVED FOR RELEASE: 2007/02/08: CIA-RDP82-00850R000300010007-0

of a turbulent mixed layer with a sharp density gradient at the discontinuity advancing within the undisturbed fluid. In most studies the authors have determined the rate of entrainment of the undisturbed fluid, the dependence of the thickness of the mixed layer of fluid (h) on time. The decisive parameters in the problem of deepening of the mixed layer are the global Richardson number $Ri_0 = h^2N^2/U_0^2$, the Prandtl number $Pr = \nu/\chi$ (or the Schmidt number, if the stratification is saline $Sc = \nu/k_S$), the Reynolds number $Re = U_0h/\nu$ or the Péclet number U_0h/χ (here U_0 is characteristic velocity, h is the scale in which velocity changes, ν is viscosity, χ is thermal conductivity, k_S is the coefficient of salt diffusion).

The greatest number of experiments involving deepening of the mixed layer were carried out using an oscillating grid fabricated from square [5, 6] or circular [7] rods and perforated plates [8]. The depth h of the mixed layer, advancing within a fluid with a constant density gradient, increases with time as $h = c(\omega_p^3 t/N^2)^n$ (here ω_p is the frequency of grid oscillation, c is a constant). The exponent n is dependent on the type of the turbulence-generating grid and the type of stratification. For example, in [8] with the destruction of temperature stratification it was found that n = 0.4 [8], whereas in [6] with the destruction of saline stratification -- n = 0.14 [6]. The forming internal waves can carry a considerable fraction of the imparted mechanical energy; in this case the rate of entrainment decreases substantially [6]. The rate of deepening of the mixed layer $U_e = dh/dt$, normalized to some characteristic velocity U_0, is a power function of the global Richardson number $Ri_0 = N^2/\overline{l^2}/\overline{U^2}$; $U_0/\overline{U} = Ri^{-m}$ (here l is the characteristic scale of turbulence; $\overline{U}$ is the mean square value of the horizontal component of turbulent velocity); m = 1 for temperature stratification, m = 1.5 for saline stratification [2]; according to data in [6] m varies from 1.5 to 0.7 with an increase in distance from the grid. The boundary of the layer becomes sharper with an increase in the Péclet number.

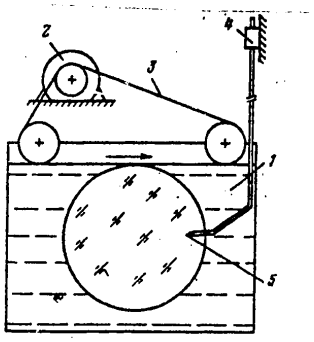

Fig. 1. Diagram of laboratory apparatus.

With propagation of the turbulent layer created by shearing stress at the upper boundary of the circular basin the rate of entrainment, normalized to the friction rate $U_+ = (\tau_*/\rho)^{1/2}$ (τ_* is frictional stress), is

APPROVED FOR RELEASE: 2007/02/08: CIA-RDP82-00850R000300010007-0

APPROVED FOR RELEASE: 2007/02/08: CIA-RDP82-00850R000300010007-0

inversely proportional to the Richardson number, $U_e/U_+ = 2.5\ Ri_*^{-1}$ with $30 < Ri_* < 300$, and the thickness h of the mixed layer increases with time, $h = U_+(15t/N_0^2)^{1/3} \sim t^{1/3}$ [3]. The mean velocity of movement of the fluid changes most rapidly at the surface of the fluid and near the interface.

The dependence of the rate of entrainment on the global Richardson number $U_e/U_+ \sim Ri_0^{-1}$ is maintained in a case when a velocity shear is created by injection and removal of fluid in the circular channel [4], and also when the source of energy and shearing is an air flow over a basin with a stratified fluid [9]. With deepening of the turbulent layer in a two-layer fluid $H\Delta\rho = H_0\Delta\rho_0$ the interface becomes sloping, the angle of slope S decreases inversely proportionally to the Richardson number $\bar{S} = 5.4 \cdot 10^{-4}\ Ri^{-1} = 5.4 \cdot 10^{-4}\ (\rho_0 U_+^2/g\Delta\rho H)$. Here H is the thickness of the upper layer, $\Delta\rho$ is the difference in densities [10]. Since in the studies which have been made for the most part there was a study of the mean characteristics of the mixed layer, it is of interest to study its spatial structure, especially in the range of values of the global Richardson number close to unity, when turbulence is created by the shearing stress at the upper boundary and in the fluid both a mean flow and turbulence are observed.

1. Experimental method. A diagram of the experimental apparatus is given as Fig. 1. Before the onset of the experiments a laboratory basin 1 with the length $l_x = 40$, with the width $l_y = 15$ and the height $l_z = 30$ cm was filled with a fluid with a constant density gradient (a water solution of NaCl with a variable concentration). The side walls of the basin were fabricated of optical glass, which makes it possible to study the pattern of flow by means of shadow methods. A shearing stress is created in the fluid by movement of a reinforced rubber belt 3 along the free surface; this is driven into motion by a synchronous motor 2 of the RD-9 type. The area of contact between the belt and the fluid is 30 x 10 cm.

In order to make the flow visual we used an IAB-451 shadow instrument with a flat slit in the illumination part and a flat blade in the receiving part. The shadow image was registered by the method of a frame-by-frame survey with an RFK-5 camera. Fluctuations of electric conductivity were measured by the pulsed sounding method; the diameter of the central electrode of the single-electrode contact converter is d = 0.5 mm [11]. The movement mechanism 4, mounted over the basin, made it possible to carry out measurements at any point in the basin 5. The scale of density change and the period of internal oscillations $T_0 = 2\pi/N$ were determined from measurement of the frequency of oscillations of the internal waves arising during sinking of the wake behind a floating-up gas bubble [12] and were $\lambda = 670$; 1,300 cm; $T_0 = 5.2$; 7.2 sec respectively. The rates of movement of the belt varied in the range from 1.2 to 17.7 cm/sec.

2. Turbulent mixed layer. Figure 2 shows a series of shadow kinograms of the pattern of flow forming during movement of the belt at a high speed ($U_0 = 17.7$ cm/sec, $\lambda = 670$ cm). The blade and slit of the shadow instrument

APPROVED FOR RELEASE: 2007/02/08: CIA-RDP82-00850R000300010007-0

APPROVED FOR RELEASE: 2007/02/08: CIA-RDP82-00850R000300010007-0

were oriented vertically; the changes in blackening density are caused by fluctuations of the horizontal component of the refraction coefficient.

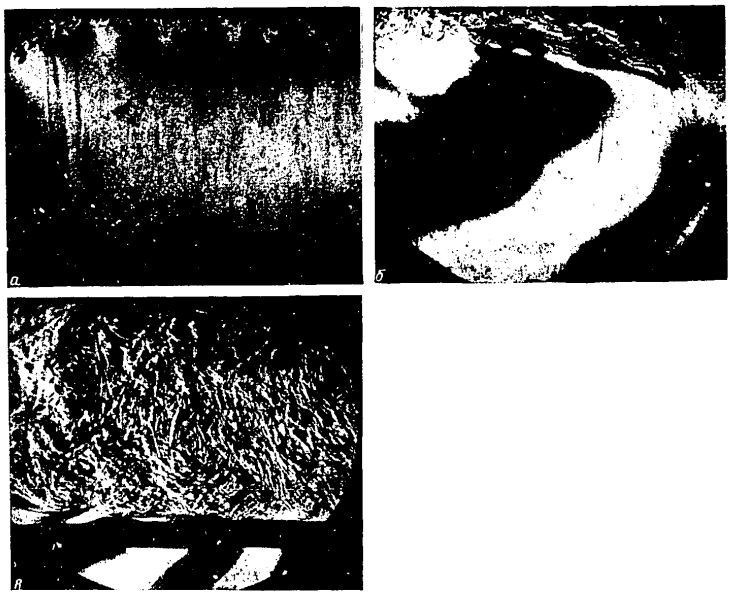

Fig. 2. Shadow picture of flow. U_0 = 17.7 cm/sec, λ = 670 cm, T = 5.2 sec: a) t = 6 sec, b) t = 20 sec, c) t = 40 min

With activation of the mechanism for movement of the belt (the time constant for the entire mechanical system is t_m = 0.2 sec, movement from left to right) in a thin layer near the surface of the fluid there is formation of a shear flow with a significant vertical gradient of the horizontal component of current velocity $\partial U_x / \partial z$. As a result of the hydrodynamic instability of the flow, along the surface of the belt there is formation of a system of eddy "ridges" whose number and size increase rapidly (Fig. 2,a, t = 6 sec). These eddy formations after 20 sec merge and form a turbulent boundary layer. Due to the surge the lighter, partially mixed fluid is accumulated in the right part of the basin and the lower surface of the mixed layer becomes sloping (Fig. 2,b, t = 20 sec). In addition to turbulence, a mean flow exists in the layer -- the fluid entrained by the belt moves from left to right, turns downward at the right wall of the basin and flows from right to left near the sloping lower boundary. The lower boundary of the turbulent layer is relatively smooth. The maximum dimension of the inhomogeneities is d = 0.2-0.6 cm, which is appreciably less than the mean

APPROVED FOR RELEASE: 2007/02/08: CIA-RDP82-00850R000300010007-0

APPROVED FOR RELEASE: 2007/02/08: CIA-RDP82-00850R000300010007-0

thickness of the layer (the thickness of the layer in the middle of the basin) h = 3.0 cm and its minimum thickness h = 1.7 cm.

The formation of the turbulent layer is accompanied by the excitation of the internal waves. The boundaries of the dark and light bands in the lower part of the photograph pass along the crests and troughs of the waves. The length of the most clearly expressed waves is λ = 8.5-12 cm. The frequency ω and the angle of slope of the wave crests to the horizon φ decrease with propagation of the waves within the basin and accordingly there is an increase in the angle of slope of the wave crests ϑ to the vertical, $\vartheta = \pi/2 - \varphi$. For example, with z = 8 cm, ω = 0.90 sec^{-1}, we have ϑ = 41°, φ = 49°, but with z = 14 cm, ω = 0.25 sec^{-1}, we have ϑ = 78°, φ = 12° (Fig. 2,b). Short waves are excited which satisfy the dispersion expression $\omega = N \cos \vartheta$. The group velocity and the energy flux in these waves are directed along the wave troughs and crests respectively from the mixed layer within the undisturbed fluid.

With the broadening of the turbulent layer there is a decrease in the angle of slope of the boundary of the zone of turbulent movement toward the horizon; $tg\ S = 0.058\ Ri_0^{-0.4}$. Turbulent mixing evens out the density within the mixing layer and on its lower boundary there is formation of a density jump layer with a high value of the density gradient $\partial\rho/\partial z$, which leads to the appearance of a black horizontal band at the lower boundary of the layer (Fig. 2,c, t = 40 min).

Data from photometric measurements of the shadow kinograms using an IFO-451 microphotometer show that the maximum of the density gradient is on the upper part of the jump layer; its lower part is more diffuse. In the stage of turbulent entrainment with $t/T_0 = \tau > 50$ the ratio of the thickness of the jump layer h_0 to the thickness of the homogeneous layer D remains constant, h_0/D = 0.33.

Within the mixed layer during the entire time of operation of the belt there is circulatory turbulent flow. The maximum velocity U_x and shear $\partial U_x/\partial z$ (Fig. 2,c) are observed in the upper part of the layer under the surface of the belt where the optical inhomogeneities (schlieren) are drawn out in a horizontal direction. In the central part of the layer, in a zone of weak convective flow, the schlieren are oriented vertically. A turbulent counterflow is formed in the lower part; the schlieren are oriented in a horizontal direction and form eddy structures. The appearance of schlieren is attributable to the fact that the particles of the inflowing fluid slowly lose their initial salinity and are drawn out into thin jets in the direction of the mean flow. The zone of turbulent mixing touches the density jump layer in the right part of the basin, where the descending surge current turns, and departs from it in the left part, where the current turns upward. The formation of internal waves in this stage is associated with the passage of large eddies near the jump layer (Fig. 2,c, t = 40 min, λ = 5.6-7.3 cm, ω = 0.84 sec^{-1}, ϑ = 46°).

APPROVED FOR RELEASE: 2007/02/08: CIA-RDP82-00850R000300010007-0

APPROVED FOR RELEASE: 2007/02/08: CIA-RDP82-00850R000300010007-0

Figure 3 shows the dependence of the mean thickness of the mixed layer, normalized to the scale of density change, $h_* = h/\Lambda$ on dimensionless time τ. On curves 1, 2 it is possible to discriminate three characteristic segments -- the initial stage of formation of turbulence, $\tau < 10$, when $h_* \sim \tau$; the stage of formation of the circulation current, $10 < \tau < 50$, when the thickness of the layer virtually does not change; the stage of turbulent entrainment, $\tau > 50$, $h_* = A\tau^{0.25}$, $A_1 = 4 \cdot 10^{-3}$ cm, $U_0 = 17.7$ cm/sec; $A_2 = 3 \cdot 10^{-3}$ cm, $U_0 = 12.0$ cm/sec, which is continued until the turbulent layer fills the entire basin. With the closing of the circulation current the lighter fluid from the near-surface layer is below the heavier fluid from the lower-lying layers; within the layer there is intensive mixing on which is expended a considerable fraction of the mechanical energy imparted to the fluid by the belt. The extent of the mixing layer is stabilized and in the course of 2 or 3 minutes its boundary does not advance within the undisturbed fluid. After the density distribution evens out within the mixing layer the undisturbed fluid again begins to be entrained into movement and the thickness of the turbulent layer increases. The rate of entrainment $U_e = dh/dt$ is not a simple power function of the Richardson number, but in the stage of turbulent entrainment, with $\tau > 120$, since $h = A\tau^{0.25}$, with allowance for determination of Ri_0 we have $U_e = A^4N^4/8\pi U_0^3 Ri_0^{3/2}$. The global Richardson number $Ri_0 = N^2h^2(t)/U_0^2$ is determined from the undisturbed frequency of oscillations N, the rate of movement of the belt U_0 and the mean thickness of the layer h(t). The nature of the dependence $U_e \sim Ri_0$ coincides with that observed in experiments with deepening of the turbulent layer created by an oscillating grid in a fluid with a saline stratification [2]. The absolute rates of entrainment are small: $U_e = (1\text{-}5) \cdot 10^{-3}$ cm/sec.

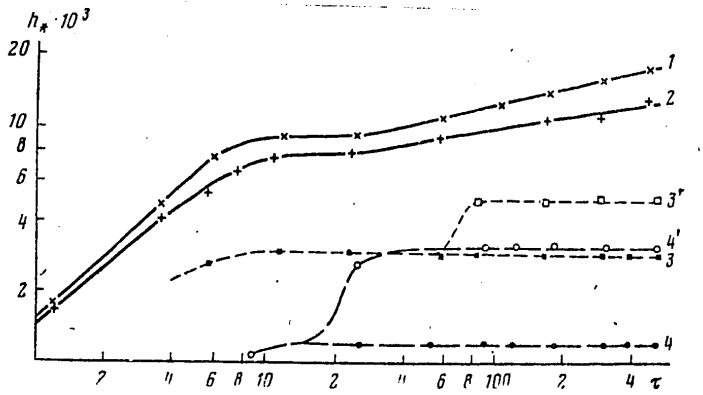

Fig. 3. Dependence of thickness of the mixed layer $h_* = h/\Lambda$ on time τ: 1-3) $\Lambda = 670$ cm, T = 5.2 sec, $u_0 = 17.7$, 12, 2.0 cm/sec, 4) $\Lambda = 1300$, T = 7.2 sec, $u_0 = 2.4$ cm/sec, 3', 4' - $h_* = H/\Lambda$.

APPROVED FOR RELEASE: 2007/02/08: CIA-RDP82-00850R000300010007-0

APPROVED FOR RELEASE: 2007/02/08: CIA-RDP82-00850R000300010007-0

Some of the energy of the turbulent layer is expended on the excitation of irregular internal waves in the lower part of the basin, in the zone of a constant density gradient. For the most part it is short internal waves which are excited; their characteristic length is 2-12 cm, angular frequency ω = 0.08-0.9 sec^{-1}, period T = 78-7 sec. The wave crests are slanted at an angle ϑ = 87-42° to the vertical (according to data from shadow photographs). The principal wave source is zones of turning of the circulation current along the lateral walls of the basin (see Fig. 2, b) and eddy formations moving along the boundary of a zone with a high density gradient in the lower part of the layer. With deepening of the mixed layer the second source becomes the most important, the length of the excited waves decreases and the frequency increases (see Fig. 2,c). Measurements of particle tracks indicated that the horizontal displacements of particles (2-3 cm) are 10-15 times greater than the vertical displacements and decrease with increasing distance from the mixed layer.

Measurements of particle displacements at the center of the basin at a depth of 25 cm, carried out using a conductivity sensor, indicated that wave disturbances have an irregular character, are observed as high-frequency waves $T \sim T_0$ with a low amplitude (A = 0.05-0.1 mm) and as more clearly expressed low-frequency oscillations T = 20-50 sec, A = 0.5-2 mm.

Laminar mixed layer. Figure 4 shows a shadow picture of a current forming when there are low rates of belt movement (U_0 = 2.4 cm/sec, λ = 670 cm, movement from left to right). The vertical lines in Fig. 4 are density marks formed by the wake behind a floating-up gas bubble. The vertical distribution of the horizontal component of the fluid current was determined by measurement of displacement of the center of the mark during a known time interval.

At the beginning of movement a laminar boundary layer is formed near the belt surface. Near the right wall, where the lighter fluid is accumulated as a result of the surge, a countercurrent begins to form and after t = 40-60 sec a closed eddy circulation layer with a sloping lower boundary is formed near the belt. Within the layer, together with the circulation current there is a convective current (Fig. 4,a) gradually evening-out the density. Zones of turning of the current and individual eddies are a source of formation of short internal waves with the parameters λ = 3-8 cm, ϑ = 50-60°, ω = 0.8-1.6 sec^{-1}, Gradually a density jump layer begins to form on the sloping lower boundary; this leads to the formation of a narrow dark band (Fig. 4,a). An undisturbed more saline fluid from the lower-lying layers flows into the mixed layer in the form of individual thin jets (schlieren) with a diameter of 1-2 mm, which are drawn out in the direction of the mean flow. In this stage there is a degeneration of the closed eddy currents within and at the boundary of the layer; the perturbations of the interface have a smooth, wavelike character and there is a decrease in the length of the forming internal waves: λ = 2-5 cm, ϑ = 40-50°, ω = 0.7-0.8 sec^{-1}.

APPROVED FOR RELEASE: 2007/02/08: CIA-RDP82-00850R000300010007-0

APPROVED FOR RELEASE: 2007/02/08: CIA-RDP82-00850R000300010007-0

After closing of the current, evening-out of density in the near-surface layer and formation of the sloping lower boundary with a great density layer, under the upper circulation layer a second eddy layer begins to form in which the rotation of the fluid occurs in the same direction (clockwise) as in the near-surface layer. As a result of the partial mixing of the fluid a density jump layer is also formed at its lower boundary and this has a rigorously horizontal orientation (Fig. 4,b). The displacements of the density mark show that in zones of maximum density change the velocity shear value U_x is maximum. The flow velocity of the fluid does not become equal to zero at the lower boundary of the second layer.

The detailed structure of the layers is shown in Fig. 4,b,c. Here the blade and slit have a horizontal orientation and the changes in blackening density on the photograph are caused by the difference $\partial n/\partial z$ (and $\partial\rho/\partial z$ respectively) from the initial values (in Fig. 4,b the belt movement is from left to right, 4, c -- from right to left). In order to investigate the pattern of flow near the wall, in the basin in the field of view of the shadow instrument a vertical plate has also been introduced; it does not quite reach to the belt. The structure of the density jump layers is nonuniform along the basin. In the surge zone the $\partial n/\partial z$ and $\partial\rho/\partial z$ values in the upper layer are maximum; the position of the boundary (layer of $\partial\rho/\partial z$ maximum) gradually changes. The boundary of the layer fluctuates and individual eddies are formed there (Kelvin-Helmholtz instability); these attenuate rather rapidly with movement along the jump layer. The characteristic scale of the inhomogeneities is h = 1 cm; the amplitude of the pulsations is A = 0.2-0.5 cm. With approach to the opposite wall of the basin in the outflow zone $\partial n/\partial z$ and $\partial\rho/\partial z$ decrease, and near the wall the boundary becomes diffuse so that individual small jets of fluid can flow from layer to layer. On the other hand, the density gradient at the lower boundary of the second layer has a minimum value near the surge zone; the width of the density jump layer here is also minimum. In this region there is a minimum difference in densities $\Delta\rho$outside and within the layer and here the fluid can flow into the lower layer. Near the zone of underflow into the upper layer the density gradient at the boundary of the lower layer becomes maximum.

The dependence of the thickness of the upper layer $h_* = h/\Lambda$ and the total thickness of both laminar layers H on time is shown in Fig. 3 (curves 3 -- U_0 = 2.0 cm/sec, Λ = 670 cm; curves 4 -- U_0 = 2.4 cm/sec, Λ= 1300 cm). With closing of the circulation current the rate of entrainment into the first layer is maximum and is $U_e = (5\text{-}6)\cdot10^{-2}$ cm/sec, t = 1 min. After formation of the second layer the current pattern is stabilized and the thickness of the circulation layers does not change. Over a period of 2-4 hours the rate of entrainment does not exceed (10^{-4}-10^{-5}) cm/sec. The change in the thickness of the layers is related to the processes of formation of the structure of the density gradient layer at the lower boundary of the current zone (the thickness of the layer was determined from the position of the middle of the layer with the maximum density gradient). The formation of the second circulation current under

APPROVED FOR RELEASE: 2007/02/08: CIA-RDP82-00850R000300010007-0

APPROVED FOR RELEASE: 2007/02/08: CIA-RDP82-00850R000300010007-0

the sloping boundary of the upper layer, rotation in which occurs in the same direction as in the upper layer, can be attributed to the effect of the following mechanism (Fig. 5).

Fig. 4. Shadow picture of current U_0 = 2.1 cm/sec, λ = 670 cm, I = 5.2 sec: a) t = 1.5 min, blade and slit vertical; b,c) t = 20 min, blade and slit horizontal, movements in different directions.

APPROVED FOR RELEASE: 2007/02/08: CIA-RDP82-00850R000300010007-0

APPROVED FOR RELEASE: 2007/02/08: CIA-RDP82-00850R000300010007-0

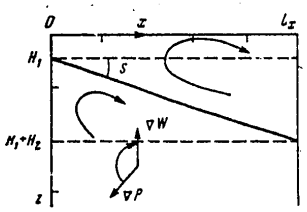

Fig. 5. Diagram of formation of second layer.

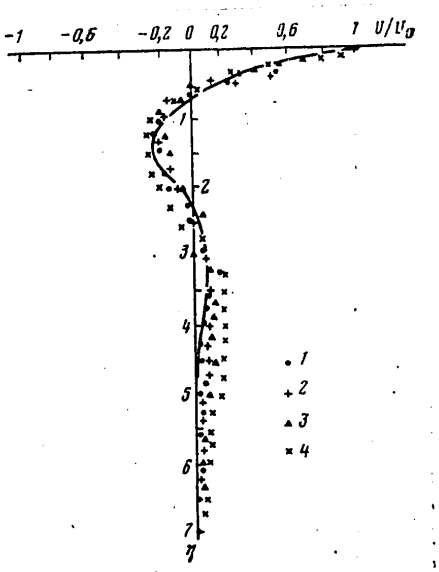

Fig. 6. Distribution of velocity with depth: 1) λ = 1,300 cm, U_0 = 1.2 cm/sec, x = 12.5 cm; 2) same with x = 18 cm; 3) λ = 900 cm, U_0 = 1.4 cm/sec; 4) λ = 900 cm, U_0 = 1.6 cm, x = 10 cm

APPROVED FOR RELEASE: 2007/02/08: CIA-RDP82-00850R000300010007-0

APPROVED FOR RELEASE: 2007/02/08: CIA-RDP82-00850R000300010007-0

Assume that the initial distribution of the fluid in an undisturbed state has the form $\rho(z) = \rho_0(1 + \Lambda^{-1}z)$, the z-axis is directed downward. Then in the approximation of a constancy of the width and the slope of the lower boundary of the near-surface layer the mean density of the fluid within it ρ_1 has the form (assuming that density does not change along y)

$$\rho_1 = \rho_0\left\{1+\frac{\Lambda^{-1}}{H^2}\left[\frac{1}{3}\left(\frac{H_2^3-H_1^3}{2H_1+H_2}\right)+H_1H_2\right]\right\} = \rho_0(H_1)+\frac{\rho_0\Lambda^{-1}}{3H_2}\left(\frac{H_2^3-H_1^3}{2H_1+H_2}\right), \quad (1)$$

where $H_2 = l_x$ tg S, S is the slope of the lower boundary; $\rho(H_1)$ is the density of fluid in an undisturbed state at the depth H_1; $H_1 + H_2$ is the maximum width of the near-surface layer. Since in the upper layer, even in a laminar flow regime, there is strong mixing, it can be assumed that $\rho(z) = \rho_1$ everywhere within it. From the condition of stability of the fluid at the discontinuity:

$$\rho_0(H_1) \geqslant \rho_1. \quad (2)$$

It follows from (1) and (2) that

$$(H_2^3-H_1^3)/(2H_1+H_2) \leqslant 0, \quad (3)$$

or

$$\rho_1 = \rho(H_1) - B,$$

where

$$B = \frac{\rho_0\Lambda_0^{-1}}{3H_2}\left(\frac{H_1^3-H_2^3}{2H_1+H_2}\right) \geqslant 0. \quad (4)$$

The difference in hydrostatic pressures at the depth H at two points $x_1 = 0$, $x_2 = x$, situated at the same depth, $\Delta P = P(x) - P(0)$ has the form:

$$\Delta P(x) = 0 \text{ when } H \leqslant H_1,$$

$$\Delta P(x) = \begin{cases} -gx\,\mathrm{tg}\,S(B+{}^1/_2\rho_0\Lambda^{-1}x\,\mathrm{tg}\,S) & \text{when } H_1+x\,\mathrm{tg}\,S<H<H_1+H_2, \\ -g(H-H_1)[B+{}^1/_2\rho_0\Lambda^{-1}(H-H_1)] & \text{when } H<x\,\mathrm{tg}\,S+H_1<H_1+H_2, \\ -gx\,\mathrm{tg}\,S(B+{}^1/_2\rho_0\Lambda^{-1}x\,\mathrm{tg}\,S) & \text{when } H>H_1+H_2. \end{cases}$$

With $z > H_1$ at any horizon $\partial P/\partial x < 0$, and since under the sloping boundary the isopycnic surfaces are oriented horizontally, from the Bjerknes theory it follows that under the sloping boundary there should be formation of a circulation current whose direction of rotation is determined by the direction of the arrow from the pressure gradient to the gradient of specific volume [13] (Fig. 5). Partial mixing within the second layer leads to the formation of a second horizontal jump layer so that the thicknesses of the upper and lower layers are approximately equal. But the current velocity at the lower boundary of the jump layer is different from zero.

APPROVED FOR RELEASE: 2007/02/08: CIA-RDP82-00850R000300010007-0

APPROVED FOR RELEASE: 2007/02/08: CIA-RDP82-00850R000300010007-0

Table 1

A, см	T, с 1	U_0, см/с 2	Время с начала движения ленты, 3 мин	Толщина верхнего слоя, h, см 4	$Re = U_0 h/\nu$	$Ri = N^2h^2/U_0^2$	Режим течения 5
670	5,2	17,7	0,1	1,2	2120	0,01	Однослойный 6
670	5,2	12,0	0,1	0,5	600	0,01	
670	5,2	7,5	1	2,0	1500	0,1	Переходный 7
1300	7,2	5,0	1	1,8	900	0,3	
1300	7,2	2,4	1	1,4	340	0,3	Двухслойный 8
670	5,2	2	1	1,9	380	1,3	
670	5,2	1,8	1	2,0	360	1,8	

KEY:

1. T, sec
2. U_0, cm/sec
3. Time from beginning of motion of belt, minutes
4. Thickness of upper layer h, cm
5. Current regime
6. Single layer
7. Transitional
8. Two-layer

The density marks method makes it possible to determine the distribution of the horizontal components of current velocity along the vertical z for different values of the longitudinal coordinate x. Figure 6 shows the dependence of the relative current velocity U_x/U_0 on the dimensionless coordinate $\eta = (z/x^{0.25})\ (g\lambda^{-1}/U_0\nu)^{0.25}$ for different x values. The solid curve represents the computed distribution of current velocity behind the leading edge of a semi-infinite plate slowly moving in a viscous stratified fluid [14]. The results of the computations satisfactorily coincide with experimental data if as the argument of the function $U_x/U_0 = f(k\eta)$ we select $k = 1.8$. The contribution of the wave component to the distribution of velocities does not exceed 5-10%. In the two-layer regime, for the most part, there is excitation of short waves with a low amplitude $A \leqslant 0.5$ mm.

4. Current regimes. With an increase in the velocity of movement of the belt there is an increase in the intensity of mixing in the lower layer and the boundary between the layers, according to data from shadow observations, becomes difficult to distinguish. However, since the movement in the layers is not turbulent, this regime can be called transient.

The results of this series of experiments for investigation of the current regimes are cited in the table.

The table shows that when $Ri_0 < 0.1$ the moving belt creates a turbulent layer; when $0.1 < Ri_0 < 0.3$ there is a transient regime; when $Ri_0 > 0.3$ there is formation of a regular true two-layer circulation current.

APPROVED FOR RELEASE: 2007/02/08: CIA-RDP82-00850R000300010007-0

APPROVED FOR RELEASE: 2007/02/08: CIA-RDP82-00850R000300010007-0

These experiments show that the spatial structure of the currents excited in the stratified fluid by the velocity shear at the free surface changes essentially with an increase in velocity.

In the case of small shearing stresses, when $Ri_0 > 0.3$, there is formation of a stationary two-layer circulation current with an identical direction of rotation of the fluid and a sloping interface between the layers. The density gradient value is maximum at the interfaces. The lower boundary of the current is horizontal; the rate of entrainment is virtually equal to zero.

In the case of great shearing stresses $Ri_0 < 0.1$ there is formation of a turbulent mixed layer whose thickness is not a monotonic function of dimensionless time τ. In the initial stage $h \sim \tau$, which coincides with the dependence of layer thickness on time in a model of formation of turbulence by the mean flow with a velocity shear [15]. Then in the course of some time the thickness of the layer virtually does not change, but in the main stage with $\tau > 50$ increases proportionally to $\tau^{0.25}$, which is close to the computed regime of deepening of the layer due to the diffusion of turbulence $h \sim t^{1/3}$ [16]. Accordingly, the rate of entrainment $U_e = dh/dt$ decreases with an increase in time, with $\tau > 50$ $U_e \sim Ri_0^{-3/2}$. The main density change occurs on the horizontal lower boundary of the layer. The process of entrainment of the fluid occurs due to interaction between the turbulent eddies and the interface. Within the undisturbed fluid there is radiation of short internal waves whose length is determined by the dimension of the generating eddies.

BIBLIOGRAPHY

1. Fedorov, K. N., TONKAYA TERMOKHALINNAYA STRUKTURA VOD OKEANA (Fine Thermohaline Structure of Waters in the Ocean), Leningrad, Gidrometeoizdat, 1976.

2. Terner, Dzh., EFFEKTY PLAVUCHESTI V ZHIDKOSTYAKH (Buoyancy Effects in Fluids), Moscow, "Mir," 1977.

3. Kato, H., Phillips, O. M., "On the Penetration of a Turbulent Layer into Stratified Fluid," J. FLUID MECH., 37, Pt 4, 643-655, 1969.

4. Moore, M. T., Long, R. R., "On Experimental Investigation of Turbulent Stratified Shearing Flow," J. FLUID MECH., 49, Pt 4, 635-655, 1971.

5. Hopfinger, E. T., Toly, T. A., "Turbulent Mixing Across Density Interface," J. FLUID MECH., 78, Pt 1, 155-177, 1978.

6. Linden, P. F., "The Deepening of a Mixed Layer in a Stratified Fluid," J. FLUID MECH., 71, Pt 2, 385-405, 1975.

APPROVED FOR RELEASE: 2007/02/08: CIA-RDP82-00850R000300010007-0

APPROVED FOR RELEASE: 2007/02/08: CIA-RDP82-00850R000300010007-0

7. Thompson, S. M., Turner, M. S., "Mixing Across an Interface Due to Turbulence Generated by an Oscillating Grid," J. FLUID MECH., 67, Pt 2, 349-368, 1975.

8. Voropayev, S. I., "Development of the Mixed Layer in a Stratified Fluid. Laboratory Experiment," MEZOMASSHTABNAYA IZMENCHIVOST' POLYA TEMPERATURY V OKEANE (Mesoscale Variability of the Temperature Field in the Ocean), Moscow, In-t Okeanologii AN SSSR, 140-152, 1977.

9. Wu, T., "Wind Induced Turbulent Entrainment Across a Stable Density Interface," J. FLUID MECH., 61, Pt 2, 275-287, 1973.

10. Wu, T., "A Note on the Slope at a Density Interface Between Two Stably Stratified Fluids Under Wind," J. FLUID MECH., 61, Pt 2, 275-287, 1973.

11. Levtsov, V. I., Chashechkin, Yu. D., "Measurement of the Conductivity of a Fluid by the Pulsed Sounding Method," TEZISY DOKLADOV III VSESOYUZNOGO SEMINARA-SOVESHCHANIYA "METROLOGIYA V RADIOELEKTRONIKE" (Summaries of Reports at the Third All-Union Seminar-Conference on "Metrology in Radioelectronics"), Moscow, VNIIFTRI, 188-189, 1975.

12. Nekrasov, V. N., Chashechkin, Yu. D., "Measurement of Current Velocity and the Period of Internal Oscillations of a Fluid by the Density Marks Method," METROLOGIYA (Metrology), No 11, 19-23, 1974.

13. Kochin, N. Ye., Kibel', I. A., Roze, N. V., TEORETICHESKAYA GIDROMEKHANIKA (Theoretical Hydromechanics), Part I, Moscow, Fizmatgiz, 1963.

14. Martin, S., Long, R. R., "The Slow Motion of a Flat Plate in Viscous Stratified Fluid," J. FLUID MECH., 31, Pt 4, 669-688, 1968.

15. Kalatskiy, V. I., "Some Analytical Solutions of the Equation of the Balance of Turbulent Energy," IZV. AN SSSR, FAO (News of the USSR Academy of Sciences, Physics of the Atmosphere and Ocean), 10, No 8, 900-904, 1974.

16. Garnich, N. G., Kitaygorodskiy, S. A., "Rate of Deepening of the Quasi-homogeneous Layer," IZV. AN SSSR, FAO, 13, No 12, 1287-1296, 1977.

COPYRIGHT: Izdatelstvo "Nauka," "Izvestiya AN SSSR, Fizika atmosfery i okeana," 1980

[269-5303]

5303
CSO: 1865

APPROVED FOR RELEASE: 2007/02/08: CIA-RDP82-00850R000300010007-0

APPROVED FOR RELEASE: 2007/02/08: CIA-RDP82-00850R000300010007-0

UDC 551.466.326

RESTORATION OF SEA WAVE SPECTRA FROM MEASUREMENTS WITH MOVING SENSORS

Moscow IZVESTIYA AKADEMII NAUK SSSR, FIZIKA ATMOSFERY I OKEANA in Russian
Vol 16, No 3, 1980 pp 294-304

[Article by A. V. Kats and I. S. Spevak, Khar'kov State Scientific Research Institute of Metrology, submitted for publication 30 September 1978]

Abstract: A study was made of the correlation of frequency-angular wave spectra in uniformly moving and fixed reference systems. The authors discuss the conditions for an unambiguous restoration of a spectrum undistorted by movement. The results allow generalization for an arbitrary wave field. Limiting cases of a narrow angular wave spectrum and a low rate of movement of the sensors are examined. A scheme of restoration of the true spectrum is proposed for these cases on the basis of measurements of the rise along several trajectories.

[Text] 1. Introduction. In measurements of sea waves with a moving sensor the measured parameter, such as the surface rise $\zeta(r,t)$, contains information both on the wave field itself and on movement of the sensor. Accordingly, the question arises as to the possibility of using data from such measurements for discriminating the statistical characteristics of sea waves undistorted by motion of the sensor.

One of the most important characteristics of the random field of rises is the spatial-temporal correlation function

$$Z(\mathbf{r}, t)=\langle\zeta(\mathbf{x}, \tau)\zeta(\mathbf{x}+\mathbf{r}, \tau+t)\rangle, \qquad (1.1)$$

where x, r are two-dimensional vectors in the plane (x,y); the "<>" symbol denotes statistical averaging (the waves are assumed to be statistically uniform and stationary). If the sensor measuring the rise $\zeta(x, t)$ moves along the trajectory X = R(t), then the correlation function

APPROVED FOR RELEASE: 2007/02/08: CIA-RDP82-00850R000300010007-0

APPROVED FOR RELEASE: 2007/02/08: CIA-RDP82-00850R000300010007-0

$$Z_R(\mathbf{r}, t)=\langle\zeta(\mathbf{x}+\mathbf{R}(\tau), \tau)\zeta(\mathbf{x}+\mathbf{R}(\tau+t)+\mathbf{r}, \tau+t)\rangle \quad (1.2)$$

is related to (1.1) by the expression

$$Z_R(\mathbf{r}, t)=Z(\mathbf{r}+\mathbf{R}(\tau+t)-\mathbf{R}(\tau), t), \quad (1.3)$$

if the R(t) trajectory is determined. (It goes without saying that under real conditions the trajectory is subject to random perturbations which in general correlate with the waves, but (1.3) will be a good approximation in the case of small perturbations.) Using (1.3), in principle it is possible to establish a correlation between the spectra

$$X(\mathbf{k}, \omega)=(2\pi)^{-3}\int d\mathbf{r}\, dt \exp(i\omega t-i\mathbf{k}\mathbf{r})Z(\mathbf{r}, t) \quad (1.4)$$

and $X_R(k, \omega)$ for an arbitrary law of motion R(t). In the case of uniform linear motion R(t) = U(t) the problem of restoration of the frequency spectrum of waves was examined in [1] for uniform waves (we note, however, that in the result cited in [1] a factor was omitted (see (2.23)). In the case of uniform motion of a sensor with a velocity substantially exceeding the wave velocity the problem was examined in [2] for one-dimensional waves.

In this study we also examine the case of a uniform linear motion of the sensor, but in contrast to [1,2], for an arbitrary (two-dimensional) wave spectrum and without restrictions on the velocity U. It is shown that in a general case, when there are both accompanying and counter waves, a precise restoration of the frequency-angular spectrum is impossible due to the appearance of an ambiguity in the Doppler frequency conversion (sec. 2). In the absence of accompanying wave components the spectrum is restored unambiguously (sec. 2). Limiting cases of small sensor velocities were considered (sec. 3), as well as a narrow angular spectrum of waves (sec. 4) when the general formulas are substantially simplified. In these limiting cases there is a discussion of restoration of the spectrum in measurements of the rise at several points [3].

2. Correlation of Frequency-Angular Wave Spectra

In the case of uniform motion the spatial-frequency spectrum $X_R(k, \omega) = X_U(k, \omega)$ is derived from $X(k, \omega)$ (1.4) by the Doppler frequency conversion $\omega \to \omega+kU$:

$$X_U(\mathbf{k}, \omega)=X(\mathbf{k}, \omega+\mathbf{k}\mathbf{U}). \quad (2.1)$$

Since the field of rises is a wave field with the dispersion law [4]

$$\omega=\omega_k=\sqrt{gk}, \quad \omega_{-k}=\omega_k, \quad (2.2)$$

the spectral density $X(k, \omega)$ is different from zero only on the dispersion surface (2.2) [5], that is

APPROVED FOR RELEASE: 2007/02/08: CIA-RDP82-00850R000300010007-0

APPROVED FOR RELEASE: 2007/02/08: CIA-RDP82-00850R000300010007-0

$$X(\mathbf{k},\omega)=\sum_{\rho=\pm1}X(\rho\mathbf{k})\delta(\omega-\rho\omega_{\mathbf{k}}). \tag{2.3}$$

[Although, strictly speaking, the dispersion equation (2.2) is correct only for waves of an infinitely small amplitude, it is a good approximation also for waves of finite amplitude if the nonlinearity is small [5].]

By virtue of the realness of the field $\zeta(x, t)$ and the postulated uniformity and stationarity $X(\mathbf{k},\omega)$ has the properties of symmetry

$$X^*(-\mathbf{k}, -\omega)=X(\mathbf{k}, \omega)=X(-\mathbf{k}, -\omega), \tag{2.4}$$

which is automatically taken into account in the representation of (2.3) with

$$X^*(\mathbf{k})=X(\mathbf{k}). \tag{2.5}$$

It follows from (2.1) and (2.3) that the spatial spectrum of waves

$$\Psi(\mathbf{k})\equiv\int_{-\infty}^{\infty}d\omega X(\mathbf{k},\omega)=X(\mathbf{k})+X(-\mathbf{k}) \tag{2.6}$$

is undistorted with a changeover to a moving reference system. It goes without saying that this is an obvious result of invariance of lengths and angles when using Galilean transformations. However, in the majority of experiments it is not the spatial spectrum which is measured, but the frequency spectrum

$$\Phi(\omega)=\int d\mathbf{k}X(\mathbf{k},\omega), \tag{2.7}$$

or the frequency-angular spectrum

$$E(\omega,\theta)=\int_{0}^{\infty}dkkX(\mathbf{k},\omega) \tag{2.8}$$

[3]; it is really possible to measure only the several first coefficients $C_n(\omega)$ of the expansion $E(\omega, \theta)$ into a Fourier series for the angle θ:

$$E(\omega,\theta)=\sum_{n=-\infty}^{\infty}C_n(\omega)e^{-in\theta},\quad C_0(\omega)=\Phi(\omega)/2\pi. \tag{2.9}$$

Thus, the $\Phi(\omega)$ frequency spectrum is the Fourier transform of the single-point correlation function Z(0,t) (see (3.1)).

By virtue of symmetry properties of (2.5) the $\Phi(\omega)$ and $E(\omega, \theta)$ functions are real

$$\Phi^*(\omega)=\Phi(\omega),\ \ E^*(\omega,\theta)=E(\omega,\theta), \tag{2.10}$$

and their negative-frequency parts contain the same information as the positive-frequency parts

APPROVED FOR RELEASE: 2007/02/08: CIA-RDP82-00850R000300010007-0

APPROVED FOR RELEASE: 2007/02/08: CIA-RDP82-00850R000300010007-0

$$\Phi(-\omega)=\Phi(\omega),\quad E(\omega,\theta)=E(-\omega,\theta+\pi). \tag{2.11}$$

As follows from (2.3), (2.7), (2.8), the X(k) spectrum contains complete information on waves. In particular,

$$E(\omega,\theta)=k\frac{dk}{d\omega_k}\sum_{\rho=\pm1}X(\rho k)\Theta(\rho\omega)\big|_{\omega_k=\omega}. \tag{2.12}$$

Accordingly, for restoration of the true frequency-angular spectrum it is necessary, using the known distorted spectrum $E_U(\omega,\theta)$

$$E_U(\omega,\theta)=\int_0^\infty dkkX_U(k,\omega) \tag{2.8a}$$

to find X(k), but $E(\omega,\theta)$ is determined using (2.8). We note that (2.12) establishes a mutually unambiguous correspondence between X(k) and $E(\omega,\theta)$

$$X(k)=X(k,\theta)=k^{-1}v_kE(\omega_k,\theta), \tag{2.13}$$

where $v_k=\partial\omega_k/\partial k$ is the group velocity of the waves; (2.8a), with (2.1) and (2.3) taken into account, in a general case cannot be solved for X(k) due to the nonmonotonic dependence of the Doppler-shifted frequency $\omega_k^U=\omega_k-kU$ on the wave number. The nonmonotonic situation (Fig. 1) arises when $kU>0$, that is, for "accompanying" waves whose phase velocity in a fixed reference system forms an acute angle with the direction of sensor movement. We will explicitly express $E_U(\omega,\theta)$ through $E(\omega,\theta)$:

$$E_U(\omega,\theta)=\sum_{\rho=\pm1}\int_0^\infty dkv_kE(\omega_k,\theta+(1-\rho)\pi/2)\delta(\omega+kU-\rho\omega_k) \tag{2.14}$$

and we will integrate (2.14), taking into account that the argument of the δ-function becomes equal to zero when $\omega_k=\sqrt{gk}\equiv\xi(\omega)$

$$\xi_\sigma^\rho(\omega)=\frac{\rho g}{2U_k}+\sigma\sqrt{\frac{g^2}{4U_k^2}-\frac{g\omega}{U_k}},\quad \sigma,\rho=\pm,\quad U_k=\frac{kU}{k},\quad k=k(\cos\theta,\sin\theta). \tag{2.15}$$

Limiting ourselves to positive frequencies, which does not lessen universality by reason of (2.11), we have

$$E_U(\omega,\theta)=\Theta(-U_k)\sum_{\rho=\pm1}\frac{E(\xi_+^\rho,\theta+(1-\rho)\pi/2)}{|1+\rho\xi_+^\rho/2\Omega|}+ \tag{2.16}$$

$$+\Theta(\Omega-\omega)\Theta(U_k)\sum_{\sigma=\pm1}\frac{E(\xi_\sigma^+,\theta)}{|1-\xi_\sigma^+/2\Omega|},\quad \omega>0,$$

where $\Omega=\Omega(\theta)=g/4|U_k|$, $\theta(x)=0$ when $x<0$ with $x<0$, $\theta(x)=1$ when $x>0$.

APPROVED FOR RELEASE: 2007/02/08: CIA-RDP82-00850R000300010007-0

APPROVED FOR RELEASE: 2007/02/08: CIA-RDP82-00850R000300010007-0

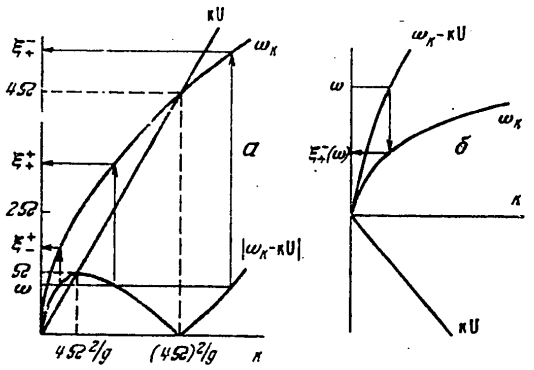

Fig. 1. Doppler frequency shift of surface waves: a) accompanying movement ($kU > 0$). A wave with the frequency ω in a moving system corresponds to two waves in a fixed system with the frequencies $\omega' = \xi_{\pm}^{+}$, symmetric relative to 2Ω; the directions of wave propagation in both systems coincide $\theta = \theta'$. With $\omega' > 4\Omega$ the frequency ω is unambiguously determined by the frequency ω' and the direction of propagation in the moving system changes to the opposite $\theta = \theta' + \pi$, b) counter waves ($kU < 0$). The transformation of frequencies is mutually unambiguous; the spectrum in the moving reference system is displaced into the high-frequency region ($\omega > \omega'$).

Waves with a phase velocity greater than the projection of sensor velocity onto the direction of wave propagation $v_{ph}(k) = \omega_k/k > U_k$ make a contribution to $E_U(\omega, \theta)$ when $\omega < \Omega$ and $kU > 0$. In this case $E_U(\omega, \theta)$ is expressed through $E(\omega', \theta)$ with $\omega' = \xi_{+}^{+} < 4\Omega$ (region II in Fig. 2, compare Fig. 1,a). For $kU < 0$ the contribution to $E_U(\omega, \theta)$ is caused by two different groups of waves: accompanying waves in a fixed reference system (region I in Fig. 2) in the direction $\theta' = \theta + \pi$ with the frequency $\omega' = \xi_{+}^{-}$ (Fig. 1,a) and counter waves, propagating in the direction $\theta' = \theta$ with the frequency $\omega' = \xi_{+}^{+}$ (Fig. 1,b, region III, Fig. 2). Since with stipulated U and θ the $E_U(\omega, \theta)$ spectrum is determined by the $E(\omega', \theta')$ spectrum at the two points ω', θ', an unambiguous restoration of the spectrum, generally speaking, is impossible. However, in special cases, for example, when accompanying waves are absent, the correlation of the spectra is unambiguous. We will examine examples.

A. Assume that the $E(\omega, \theta)$ spectrum is different from zero only in the right half-plane

$$E(\omega_k, \theta) = E_+(\omega_k, \theta)\Theta(\cos\theta), \qquad (2.17)$$

APPROVED FOR RELEASE: 2007/02/08: CIA-RDP82-00850R000300010007-0

APPROVED FOR RELEASE: 2007/02/08: CIA-RDP82-00850R000300010007-0

and the velocity of the sensor forms with the x-axis the angle $\varphi \in (\pi/2, \pi)$ (Fig. 3,a). Then an unambiguous restoration is possible in the sector I ($-\pi/2<\theta<\varphi-\pi/2$) (corresponding to region I in Fig. 2), where there are counter waves:

$$E_+(\omega, \theta)=(1+\omega/2\Omega)E_U(\omega+\omega^2/4\Omega, \theta),$$
$$0<\omega<\infty, \quad U_k=U\cos(\varphi-\theta)<0. \tag{2.18}$$

The $E_U(\omega, \theta)$ spectrum is displaced relative to $E(\omega', \theta)$ into the high-frequency region (Fig. 1,b) due to Doppler frequency conversion -- $\omega_k \to \omega_k^U = \omega_k - kU_k > \omega_k$; the possibility of restoration is governed by the monotonic nature of the dependence of ω_k^U on k when we have $kU = kU_k > 0$. For $\varphi - \pi/2<\theta<\pi/2$ (sector II) the deformed spectrum at small frequencies $\omega<\Omega$ (region II, Fig. 2) is determined by rapid accompanying waves ($v_{ph} > U_k$, $0<\omega'<4\Omega$, Fig. 1,a):

$$E_U(\omega, \theta)=\sum_{\sigma=\pm 1}\frac{E_+(\xi_\sigma^+, \theta)}{|1-\xi_\sigma^+/2\Omega|}, \tag{2.19}$$
$$\omega<\Omega, \quad 0<\xi_-^+<2\Omega<\xi_+^+<4\Omega, \quad U_k>0.$$

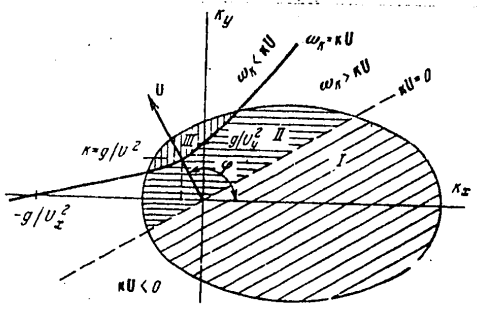

Fig. 2. Breakdown of wave field components in a moving reference system. The oblique ruling (I) represents counter waves; the horizontal ruling (II) represents rapid accompanying waves; the vertical ruling (III) represents slow accompanying waves, the direction of whose movement in a moving reference system changes to the opposite.

For an observer in a coordinate system related to the sensor both wave systems will move in the initial direction, but the group velocity of the waves, corresponding to the greater of the roots (ξ_+^+) of the dispersion equation $\omega = \omega_k - kU_k$, is less than the sensor velocity.

When $\omega = \Omega$ both roots of the dispersion equation coincide (Fig. 1,a) and the denominator in (2.19) becomes equal to zero, that is, the $E_U(\omega, \theta)$ spectrum has a singularity when $\omega = \Omega$; it occurs from waves with the frequency $\omega' = 2\Omega$. This resonance is caused by the coincidence of sensor velocity with the group velocity of the waves $v_k = \partial\omega_k/\partial k = U_k$, that is, a wave packet formed from waves with the frequencies $\omega' \approx 2\Omega$ will be fixed relative to the sensor. Oscillations of the rise in the sensor reference system occur with the frequency Ω. This singularity in the spectrum is integrable

APPROVED FOR RELEASE: 2007/02/08: CIA-RDP82-00850R000300010007-0

APPROVED FOR RELEASE: 2007/02/08: CIA-RDP82-00850R000300010007-0

$$\int_0^{\omega} d\omega E_U(\omega, \theta) = \int_0^{4\Omega} d\omega' E(\omega', \theta) \qquad (2.20)$$

and is related to the fact that the energy falling in the small frequency interval of the $E(\omega', \theta)$ spectrum near $\omega' = 2\Omega$ gives a contribution to $E_U(\omega, \theta)$ in a far narrower spectral interval $\omega \lesssim \Omega$. In actuality, it goes without saying, there will be no singularity in the $E_U(\omega, \theta)$ spectrum, since really the waves have the attenuation γ_k and the averaging time T is finite. In this case zero denominators do not arise, but small denominators, $\omega\gamma_k/\Omega$ or $1/T\Omega$, in a frequency region with the width $\Delta\omega \omega \max(\gamma, T^{-1})$; the spectral intensity increases approximately by a factor of Ω/γ or $T\Omega$ in comparison with the values in the nonresonance region. We note that the appearance of resonance can be used for measuring the spectrum in the case of accompanying movement, in any case, the possibility of formation of a maximum in $E_U(\omega, \theta)$ with $\omega = \Omega$ in the presence of accompanying waves must be taken into account when processing measurement data.

a b c

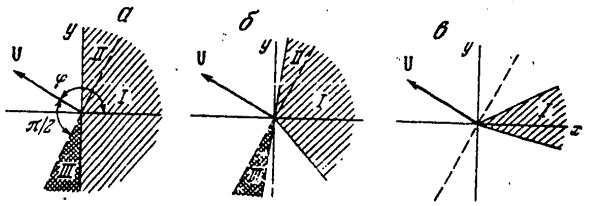

Fig. 3. Angular spectrum transformation. The simply shaded pattern is for the region of angles in which there is propagation of waves ($E(\omega, \theta) \neq 0$), the doubly shaded pattern is for the region where $E(\omega, \theta) = 0$, $E_U(\omega, \theta) \neq 0$; I) counter waves, restoration of the spectrum is unambiguous for cases a-c; II) accompanying waves, restoration in general impossible; III) registry of slow ($\omega_k > 4\Omega$) accompanying waves perceived as counter waves in a moving reference system.

At high frequencies $\omega' > 4\Omega$ in sector II the spectrum is restored unambiguously (Figures 1,a, 2, 3,a); it is related to the $E_U(\omega, \theta)$ spectrum in the sector III (Fig. 3,a):

$$E_+(\omega, \theta) = (\omega/2\Omega - 1) E_U(\omega^2/4\Omega - \omega, \theta - \pi), \quad \omega > 4\Omega. \qquad (2.21)$$

The unambiguity in restoration of the spectrum of accompanying waves is governed here by the fact that the velocity of the high-frequency waves ($\omega_k > 4\Omega$) is less than the sensor velocity and therefore in a reference system moving with the velocity U they move in the opposite direction, that is, give a contribution to $E_U(\omega, \theta)$ in sector III, not in sector II

APPROVED FOR RELEASE: 2007/02/08: CIA-RDP82-00850R000300010007-0

APPROVED FOR RELEASE: 2007/02/08: CIA-RDP82-00850R000300010007-0

(Fig. 3,a). Thus, here two factors are of importance: 1) the postulated absence of waves with directions of propagation in the left half-plane and 2) change in the direction of propagation of slow (high-frequency) waves with a changeover into a moving reference system.

In the special case of sensor movement in a negative direction of the x-axis ($\varphi = \pi$) the accompanying waves are absent and the $E(\omega, \theta)$ spectrum can be completely restored using the expression (2.18).

B. If there are waves in a sector of arbitrary width, it is possible to use the analysis carried out in example A because the only important factor is the presence or absence of accompanying waves. In particular, if waves occupy a sector with a width less than π, with such a movement of the sensor when the projections of wave velocities onto the direction of sensor movement are negative (Fig. 3,c) there can be a complete restoration of the spectrum (2.18). However, if accompanying waves are present (Fig. 3,b) the angular spectrum is singularly broadened: it is non-zero as well in region III, in which there is a contribution from the high-frequency waves from region II; in region I and for the high-frequency waves from region II the restoration is accomplished unambiguously, whereas for the low-frequency part of the spectrum of waves from region II we have only the expression (2.19).

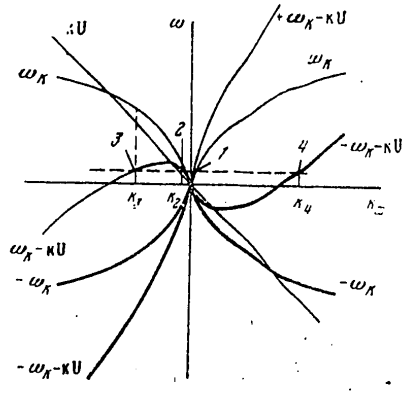

Fig. 4. Illustration of ambiguity arising in restoration of the frequency spectrum of one-dimensional waves. In general, four different wave vectors correspond to a definite value of the frequency ω. The roots of the dispersion equation are numbered. The first root corresponds to counter waves whereas the other three correspond to accompanying waves. The sensor moves in a negative direction of the x-axis.

APPROVED FOR RELEASE: 2007/02/08: CIA-RDP82-00850R000300010007-0

APPROVED FOR RELEASE: 2007/02/08: CIA-RDP82-00850R000300010007-0

C. We will examine a one-dimensional case in which we will be concerned with restoration of the frequency spectrum (2.7). Since the waves are propagated only in two opposite directions, the frequency spectrum is obtained from frequency-angular summation in these directions (θ = 0, π). Assuming for unambiguity that $U_\varphi = U\cos\varphi < 0$, from (2.16) we have:

$$\Phi_U(\omega)=\sum_\rho \frac{E(\xi_+^{\rho+},(1-\rho)\pi/2)}{|1+\rho\xi_+^{\rho+}/2\Omega|}+\theta(\Omega-\omega)\sum_\sigma \frac{E(\xi_\sigma^{+-},\pi)}{|1-\xi_\sigma^{+-}/2\Omega|}, \qquad (2.22)$$

where $\xi_\sigma^{\rho\tau}=2\Omega[-\rho\tau+\sigma\sqrt{1+\tau\omega/\Omega}]=\xi_\sigma^{\rho}|U_k=\tau U_x,\ \Omega=g/4|U_x|.$

Since the frequency spectrum does not contain information on the angular distribution of waves, the contribution to the $\Phi_U(\omega)$ spectrum at the frequency ω is, in general, from four waves (when $\omega>\Omega$— two waves) with different frequencies ω' (Fig. 4). However, in the case of presence of only counter waves ($E(\xi,\pi)$ = 0) the restoration is unambiguous. A formula for restoration of the frequency spectrum is derived from (2.18) by the substitution $E_+(\omega,\theta)\to\Phi(\omega)$:

$$\Phi(\omega)=(1+\omega/2\Omega)\Phi_U(\omega+\omega^2/4\Omega), \qquad (2.23)$$

which differs by the factor $(1+\omega/2\Omega)$ from the result obtained in [1]. [The presence of this factor ensures satisfaction of the equation

$$\int_{-\infty}^{\infty} d\omega\,\Phi(\omega)=\int_{-\infty}^{\infty} d\omega\,\Phi_U(\omega),$$

being an obvious corollary of coincidence of the correlation functions with zero arguments.]

An unambiguous restoration of the spectrum of accompanying waves (in the absence of counter waves $E(\xi,0)=0$, $E(\xi,\pi)=\Phi(\omega)$) is possible only at high frequencies $\omega>2(1+\sqrt{2})\Omega$

$$\Phi(\omega)=(\omega/2\Omega-1)\Phi_U(\omega^2/4\Omega-\omega), \qquad (2.24)$$

the lower boundary of the frequency range in which the restoration of the accompanying waves is unambiguous increases in comparison with that for the frequency-angular spectrum (compare (2.21), where $\omega>4\Omega$). For small frequencies $\omega<\Omega$ we have

$$\Phi_U(\omega)=\frac{\Phi(\xi_+^{-+})}{|1-\xi_+^{-+}/2\Omega|}+\sum_\sigma \frac{\Phi(\xi_\sigma^{+-})}{|1-\xi_\sigma^{+-}/2\Omega|}, \quad \omega<\Omega. \qquad (2.25)$$

Since in the $\Phi_U(\omega)$ spectrum with $\omega<\Omega$ the contribution is from waves of three frequencies $\omega_i'<2(1+\sqrt{2})\Omega$,

APPROVED FOR RELEASE: 2007/02/08: CIA-RDP82-00850R000300010007-0

APPROVED FOR RELEASE: 2007/02/08: CIA-RDP82-00850R000300010007-0

$$0<\xi_-^{+-}<2\Omega<\xi_+^{+-}<4\Omega<\xi_+^{-+}<2(1+\sqrt{2})\Omega,$$

then the low-frequency part of the $\Phi(\omega')$ spectrum cannot be unambiguously determined from $\Phi_U(\omega)$. The appearance of an additional ambiguity (third root ξ_+^{-+}) is related to the fact that in the frequency spectrum there is no separation of waves by directions and this root corresponds to slow waves which in the system of the sensor move in a direction opposite the initial direction. In the frequency-angular spectrum the contribution of these waves would be registered separately from the contribution of the first two in connection with a change in the direction $\theta' = \theta + \pi$. For this same reason there is a decrease in the frequency range where there can be an unambiguous restoration of the accompanying waves (high-frequency part of the spectrum).

Thus, restoration of the $E(\omega, \theta)$ spectrum from the known $E_U(\omega, \theta)$ spectrum under definite conditions is unambiguous and is accomplished using expression (2.18). However, usually such complete information on waves is lacking but the rise on several close trajectories is known [6]. [The relationship of the frequency-angular spectra of waves obtained above can be used in finding spectra having a known functional form and described by a small number of parameters (for example, see [5, 7]).] Below we will examine the procedure for restoration of the spectrum in such measurements; we will limit ourselves to limiting cases of a narrow angular spectrum and also a low velocity of the sensors. The case of movement of sensors at a great velocity will be examined separately.

In concluding this section we note that the results allow generalization for the case of arbitrary wave fields. With an increase (decrease) in phase velocity of waves with a decrease in wavelength an ambiguity in the restoration of frequency spectra arises for long (short) waves.

3. Low Velocity

In measurements of the rise at several points by fixed sensors by the use of a known method [3] it is possible to find several of the first terms in the expansion of the frequency-angular spectrum into a Fourier series with respect to the angle (2.9). In this case the $C_n(\omega)$ coefficients are expressed through the derivatives of the correlation function $Z(r,t)$ (1.1) when $r = 0$:

$$C_n(\omega)=\frac{1}{2\pi i^n}\left(\frac{g}{\omega^2}\right)^n Z^{(n)}(\omega), \quad C_{-n}(\omega)=C_n^*(\omega), \quad n=0,1,\ldots, \tag{3.1}$$

where $Z^n(\omega)$ is the frequency representation of the function

$$Z^{(n)}(t)=(\partial/\partial x+i\partial/\partial y)^n Z(r,t)\big|_{r=0}, \quad n=0,1,\ldots \tag{3.2}$$

If the system of sensors moves, the functions constructed similarly to (3.1)

APPROVED FOR RELEASE: 2007/02/08: CIA-RDP82-00850R000300010007-0

APPROVED FOR RELEASE: 2007/02/08: CIA-RDP82-00850R000300010007-0

$$E_n(\omega)=\frac{1}{2\pi i^n}\left(\frac{g}{\omega^2}\right)^n Z_U^{(n)}(\omega), \quad n=0,1,\ldots \tag{3.1a}$$

no longer are equal to the $C_n^U(\omega)$ coefficients. However, using expressions (1.5), (2.1), (2.8) it is possible to express the experimental data (3.3) through the wave spectrum:

$$U=U(\cos\varphi,\sin\varphi).$$

$$E_n(\omega)=\frac{1}{2\pi}\int_0^{2\pi}d\theta\, e^{in\theta}\int_0^{\infty}d\omega_k\left(\frac{\omega_k}{\omega}\right)^{2n}\sum_p E\left(\omega_k,\theta+\frac{1-p}{2}\pi\right)\times\delta\left[\omega+\frac{\omega_k^3U}{g}\cos(\varphi-\theta)-\omega_k\right]$$

Expanding (3.3) into a series for U and carrying out integration for the angle, we obtain a system of equations relating $E_n(\omega)$ and $C_n(\omega)$:

$$E_n(\omega)=\sum_{l=0}^{\infty}\sum_{m=0}^{l}\frac{1}{l!}\binom{m}{l}\left(\frac{U}{2g}\right)^l e^{i(2m-l)\varphi}\frac{1}{\omega^{2n}}\frac{\partial^l}{\partial\omega^l}[\omega^{2n+2l}C_{n+2m-l}(\omega)], \tag{3.4}$$

where $\binom{m}{l}$ are binomial coefficients. A solution of the system of equations (3.4) relative to C_n will be sought in the form of a series in the theory of perturbations $\omega U/g \ll 1$. In the main approximation

$$C_n^{(0)}(\omega)=E_n(\omega), \quad C_{-n}^{(0)}(\omega)=E_n^*(\omega), \quad n=0,1,\ldots \tag{3.5}$$

A formal solution with an accuracy to terms $(\omega U/g)^l$ is obtained by an l-fold iteration of (3.4), with (3.5) taken into account. Here we will cite a solution with an accuracy to second-order terms

$$C_n(\omega)=E_n(\omega)-\frac{U}{2g}\hat{L}_1[e^{i\varphi}E_{n+1}(\omega)+e^{-i\varphi}E_{n-1}(\omega)]+$$
$$+\frac{1}{2}\left(\frac{U}{2g}\right)^2\hat{L}_2[e^{2i\varphi}E_{n+2}(\omega)-e^{-2i\varphi}E_{n-2}(\omega)]+ \tag{3.6}$$
$$+\left(\frac{U}{2g}\right)^2\hat{L}_3[E_n(\omega)+e^{-2i\varphi}E_{n-2}(\omega)]+O\left[\left(\frac{\omega U}{g}\right)^3\right], \quad n=0,\pm1,\ldots,$$

$$\hat{L}_1=\omega^{-2|n|}\frac{\partial}{\partial\omega}\omega^{2|n|+2}, \quad \hat{L}_2=\omega^{-2|n|}\frac{\partial^2}{\partial\omega^2}\omega^{2|n|+4}, \quad \hat{L}_3=\omega^{-2|n|}\frac{\partial}{\partial\omega}\omega^4\frac{\partial}{\partial\omega}\omega^{2|n|},$$

where in accordance with (3.5) we will assume that $E_{-m}(\omega) = E_m^*(\omega)$, $m > 0$.

If we actually know a finite number of $E_n(\omega)$ spectra with $0 \leqslant n \leqslant k$, it follows from the structure of equations (3.4) (compare (3.6)) that it is possible to determine only 2k+1 coefficients $C_m(\omega)$ ($m = 0, \pm1, \ldots, \pm k$); In addition, the coefficients $C_{\pm(k-l)}$ ($0 \leqslant l \leqslant k$) can be determined with an accuracy to terms of the l-th order. In particular, if the rise is measured at five points arranged in the form of a cross [3, 6], then by replacing the derivatives of x, y by finite differences it is possible to find E_0, E_1, E_2 and E_3, which makes it possible to determine C_0 in the third order, $C_{\pm1}$ in the second order, $C_{\pm2}$ in the first order and $C_{\pm3}$ in the zero order with respect to $\omega U/g$.

APPROVED FOR RELEASE: 2007/02/08: CIA-RDP82-00850R000300010007-0

APPROVED FOR RELEASE: 2007/02/08: CIA-RDP82-00850R000300010007-0

4. Small-Angle Approximation

If the angular width of the spectrum $\Delta\theta$ is small ($\Delta\theta \ll 1$), with a suitable choice of the direction of velocity of the system of sensors all the waves will be counter waves and the restoration of the spectrum is unambiguous (sec. 2). In this case it is convenient to examine the angular moments $X_m(\omega)$ of the $E(\omega, \theta)$ spectrum:

$$X_m(\omega)=\frac{1}{2\pi}\int d\theta(\theta-\theta_0)^m E(\omega,\theta)\infty(\Delta\theta)^m, \quad m=0,1,\ldots, \tag{4.1}$$

where the θ_0 angle corresponds to the general direction (below we will assume that $\theta_0 = 0$). Expanding (3.3) for θ, we obtain:

$$\omega^{2n}E_n(\omega)= \tag{4.2}$$
$$\int_0^\infty d\omega_k\omega_k^{2n}X_0(\omega_k)\delta(\eta)+in\int_0^\infty d\omega_k\omega_k^{2n}X_1(\omega_k)\delta(\eta)+ U\sin\varphi/g\frac{\partial}{\partial\omega}\int_0^\infty d\omega_k\omega_k^{2n+2}X_1(\omega_k)\delta(\eta)+O[(\Delta\theta)^2],$$

where $\eta = \omega + (\omega_k^2 U/g)\cos\varphi - \omega_k$. Carrying out integration in (4.2) and separating the real and fictitious parts

$$(\omega_0/\omega)^{2n}E_n(\omega_0)=A_n(\omega)+iB_n(\omega), \tag{4.3}$$

we arrive at the equations

$$A_n(\omega)=\frac{X_0(\omega)}{\alpha}+\frac{1}{2\alpha}\frac{\partial}{\partial\omega}\left[\frac{\omega\beta_v}{\alpha}X_1(\omega)\right]+\frac{n\beta_v}{\alpha^2}X_1(\omega)+O[(\Delta\theta)^2],$$
$$B_n(\omega)=nX_1(\omega)/\alpha+O[(\Delta\theta)^2], \quad n=0,1,\ldots,l, \tag{4.4}$$

where $\beta = 2\omega U/g$, $\alpha = 1 - \beta_z$, $\omega_0 = \omega - (\omega^2 U/g)\cos\varphi$. When n = 0 the first expression in (4.4) in a zero order for $\Delta\theta \ll 1$ coincides with formula (2.23)

$$(A_0(\omega)=E_0(\omega_0)=(1/2\pi)\Phi_v(\omega),\ X_0(\omega)=(1/2\pi)\Phi(\omega)).$$

A solution of system (4.4) is sought in the form of a series for $\Delta\theta \ll 1$

$$X_m(\omega)=\sum_{i=0}^{\infty}X_m^{(i)}(\omega), \quad X_m^{(i)}\sim(\Delta\theta)^{m+i}. \tag{4.5}$$

In a zero order for $\Delta\theta$ we have for $X_0^{(0)}(\omega)$ the system

$$X_0^{(0)}(\omega)=\alpha A_n(\omega), \quad n=0,1,\ldots,l,$$

by solving which by the least squares method we obtain:

$$X_0^{(0)}(\omega)=\frac{\alpha}{l+1}\sum_{n=0}^{l}A_n(\omega)+O(\Delta\theta). \tag{4.6}$$

A solution of (4.4) can be obtained in any order for $\Delta\theta$, but the resulting expressions have an extremely unwieldy form. Here we will cite a solution in a linear approximation. Using a solution of the zero approximation, for $X_0^{(1)}$ and $X_1^{(0)}$ from (4.4) we obtain

APPROVED FOR RELEASE: 2007/02/08: CIA-RDP82-00850R000300010007-0

APPROVED FOR RELEASE: 2007/02/08: CIA-RDP82-00850R000300010007-0

$$X_0^{(1)}+\frac{1}{2}\frac{\partial}{\partial\omega}\left[\frac{\omega\beta_v^2}{\alpha}X_1^{(1)}\right]+\frac{n\beta_v}{\alpha}X_1^{(0)}=\alpha A_n^{(1)},\quad n=0,1,\ldots,l. \tag{4.7}$$

$$X_1^{(0)}=\alpha B_n/n,\quad n=1,\ldots,l, \tag{4.8}$$

where $A_n^{(1)}(\omega)\equiv A_n(\omega)-X_0^{(0)}(\omega)\infty\Delta\theta$. Excluding the function $X^{(1)}$ by means of the first of the equations (4.7) from the remaining l equations, with allowance for (4.8) we arrive at a system of $2l$ algebraic equations relative to $X_1^{(0)}$. We find a solution of this system by the least squares method:

$$X_1^{(0)}=(1/2l)(\alpha^2/\beta_v)\sum_1^l(A_n-A_0)/n+(\alpha/2l)\sum_1^l B_n/n. \tag{4.9}$$

With known $X_1^{(0)}$ the $X_0^{(1)}$ value is found as solution of equation (4.7):

$$X_0^{(1)}=-(l\beta_v/\alpha)X_1^{(0)}-{}^1/_2\partial/\partial\omega[(\omega\beta_v/\alpha)X_1^{(0)}]. \tag{4.10}$$

Formulas (4.9), (4.10), (4.6), (4.5) solve the problem of restoration of a narrow angular spectrum in a linear (with respect to $\Delta\theta\ll 1$) approximation.

BIBLIOGRAPHY

1. Zaslavskiy, M. M., Kestner, A. P., Filippov, I. A., TROPEKS-72 (TROPEX-72), Gidrometeoizdat, p 641, 1974.

2. Laykhtman, D. L., Leonov, A. I., Miropol'skiy, Yu. Z., "Interpretation of Measurements of the Statistical Characteristics of Scalar Fields in the Ocean in the Presence of Internal Gravitational Waves," IZV. AN SSSR, FAO (News of the USSR Academy of Sciences, Physics of the Atmosphere and Ocean), 7, No 4, p 447, 1971.

3. Krylov, Yu. M., SPEKTRAL'NYYE METODY ISSLEDOVANIYA I RASCHETA VETROVYKH VOLN (Spectral Methods for Investigating and Computing Wind Waves), Gidrometeoizdat, 1966.

4. Landau, L. D., Lifshits, Ye. M., MEKHANIKA SPLOSHNYKH SRED (Mechanics of Continuous Media), Gostekhizdat, 1953.

5. Fillips, O. M., DINAMIKA VERKHNEGO SLOYA OKEANA (Dynamics of the Upper Layer of the Ocean), "Mir," 1969.

COPYRIGHT: Izdatel'stvo "Nauka," "Izvestiya AN SSSR, Fizika atmosfery i okeana," 1980

[269-5303]

5303
CSO: 1865

APPROVED FOR RELEASE: 2007/02/08: CIA-RDP82-00850R000300010007-0

APPROVED FOR RELEASE: 2007/02/08: CIA-RDP82-00850R000300010007-0

UDC 551.463.5:535.31:551.46.086

ACCURACY IN MEASURING THE PARAMETERS OF THE SEA SURFACE BY OPTICAL SCATTEROMETERS AND ALTIMETERS

Moscow IZVESTIYA AKADEMII NAUK SSSR, FIZIKA ATMOSFERY I OKEANA in Russian Vol 16, No 3, 1980 pp 305-312

[Article by A. G. Luchinin, Institute of Applied Physics, submitted for publication 27 November 1978]

Abstract: Expressions are derived for random realizations, mean values and energy spectra of glitter signals in sea optical scatterometers and altimeters. On the assumption of smallness of the internal noise of the photodetector the author gives evaluations of the accuracy of measurements of the dispersion of sea surface slopes and the distance between the mean level and the altimeter.

[Text] In this article the author examines the principal properties of signals in two types of active optical systems for observing the wave-covered sea surface -- scatterometers and altimeters. It is assumed that the component of light radiation caused by volume scattering in the near-surface water layer can be neglected and the useful signal in these instruments is formed due to mirror reflection of the directed radiation from appropriately oriented surface elements.

As is well known [1-3], the useful information in scatterometers operating on the basis of glitter is in the power of the signal arriving in the detector. On the basis of its value as a function of the observation angle it is possible to judge, in particular, about the spatial distribution of the dispersion of sea surface slopes, and accordingly, about the direction and velocity of the wind over the surface [1-3], about the possibility of observing underwater objects through the wave-covered interface [4], remote detection of petroleum spots on the sea surface [1,2], etc.

With respect to altimeters, their operating principle is obvious: information on altitude is contained in the phase of the received signal (for altimeters operating with a sinusoidally modulated (SM) beam) or in the lag time of the light pulse reflected by the surface (for pulsed

APPROVED FOR RELEASE: 2007/02/08: CIA-RDP82-00850R000300010007-0

APPROVED FOR RELEASE: 2007/02/08: CIA-RDP82-00850R000300010007-0

altimeters). The use of such instruments in oceanography can be useful for studying the sea geoid and the variability of the topography of the world ocean [5].

In this connection it is important to evaluate with what accuracy it is possible to measure the dispersion of the slopes or height in the instruments enumerated above, and, in particular, answer the question as to how this accuracy is related to the state of the surface and the principal parameters of the instruments. It is evident that the accuracy of such measurements must be determined by the noise level of the detector and also the value and spectral composition of the fluctuations of the signal arriving at the detector. Since the method for computing the photodetector noise is known (for example, see [6]), and in general is dependent on its type, henceforth we will examine only the noise related to fluctuations of the optical signal itself. In case of necessity the detector noise can be easily taken into account. Therefore, the evaluation cited below pertains to any ideal observation system in which the parameters of the received signal can be registered with as high an accuracy as desired. The accuracy of the measurements in this case will be characterized by the standard deviation of these parameters (observed in a limited surface sector) from their mean values, determined on the assumption of a statistical homogeneity of the surface. The evaluation of measurement accuracy obtained in this way can be regarded as the maximum attainable.

Before proceeding to computations of fluctuations of the useful signals, we will first cite the principal formulas relating their random realizations and the mean values to the surface parameters.

1. Functional Relationships Between Parameters of Sea Surface and Radar Signals

First we will examine the properties of a signal in instruments of the scatterometer type. We will assume that the radiation source and detector are spatially matched and the optical axes of their directional diagrams coincide. In this case the detector receives radiation reflected by the surface in a backward direction and its glitter image can be formed by scanning with a narrow light beam in the case of wide-angle reception or due to use of a multicomponent detector (camera, TV receiving tube, etc.) when the surface is irradiated with a broad beam. Thereafter for simplicity and shortening the writing of the formulas we will assume that regardless of the method for forming and registering the image the time necessary for this (the time for obtaining a frame) is quite small so that the surface can be considered "frozen." For this purpose we will assume that the directional diagrams and the apertures of the source and detector are described by Gauss functions. Then the brightness of the light field I_0 at the source output and the function describing the properties of the detector D can be represented in the following form:

APPROVED FOR RELEASE: 2007/02/08: CIA-RDP82-00850R000300010007-0

APPROVED FOR RELEASE: 2007/02/08: CIA-RDP82-00850R000300010007-0

$$I_0=\frac{P_0}{\pi^2 a_{\text{п}}^2\beta_{\text{п}}^2}\exp\left\{-\frac{(\mathbf{r}-\mathbf{r}_0)^2}{a_{\text{п}}^2}-\frac{(\varkappa_\perp-\varkappa_{0\perp})^2}{\beta_{\text{п}}^2}\right\},$$

[п = detector; и = source]

$$D=\exp\left\{-\frac{(\mathbf{r}-\mathbf{r}_0)^2}{a_{\text{п}}^2}-\frac{(\varkappa_\perp-\varkappa_{0\perp})^2}{\beta_{\text{п}}^2}\right\},$$

where P_0 is the power of the source; r_0 is a vector describing the position of the scatterometer in the horizontal plane; $\varkappa_0$ is a unit vector directed along the axis of the directional diagram; $\varkappa_{0\perp}$ is its projection onto the horizontal plane; the parameters a_{source}, $a_{detector}$, β_{source}, $\beta_{detector}$ characterize the width of the apertures and the diagrams of the source and detector.

If the observation is made in directions close to the normal ($|\varkappa_{0\perp}|\ll 1$) and the height of positioning of the scatterometer above sea level is much greater than wave height, the expression for a random realization of signal power in one image element in this case has the form:

$$P=\frac{P_0 a_{\text{п}}^2 R}{\pi\beta_{\text{п}}^2 h^2(a_{\text{п}}^2+a_{\text{и}}^2)}\iint_{-\infty}^{\infty}\exp\left\{-\frac{(\mathbf{r}-\mathbf{r}_0)^2}{\beta_0^2 h^2}-\frac{4[\mathbf{r}_0-\mathbf{r}+h(\mathbf{n}_\perp-\varkappa_{0\perp})]^2}{a_{\text{п}}^2+a_{\text{и}}^2}\right\}d\mathbf{r}, \qquad (1)$$

[п = detector; и = source]

where R is the reflection coefficient ($R = 2\cdot10^{-2}$), $\beta_0^2 = \beta_{source}^2\cdot\beta_{detector}^2/(\beta_{source}^2+\beta_{detector}^2)$, $n_\perp(r)$ is the projection of the unit normal to the surface onto the horizontal plane; with the opposite sign this value is equal to the surface gradient and characterizes the value and direction of the slope at a particular surface point. In writing (1) it was assumed that $\beta_{source}^2 h^2 \gg a_{source}^2$ and $\beta_{detector}^2 h^2 \gg a_{detector}^2$.

Assuming that the surface rises have a normal distribution and assuming the waves to be isotropic, it is possible to obtain the following evaluation for the mean (for a set of surface realizations) signal power (1):

$$P=\frac{P_0 a_{\text{п}}^2\beta_{\text{п}}^2 R}{8(\beta_{\text{п}}^2+\beta_{\text{и}}^2)h^2\sigma_\theta^2}\exp\left\{-\frac{\varkappa_{0\perp}^2}{2\sigma_\theta^2}\right\}, \qquad (2)$$

where σ_θ^2 is the dispersion of slopes. In the derivation of (2) it was assumed that there is satisfaction of the inequality $\beta_0^2 \ll 2\sigma_\theta^2$. Expression (2) reflects the well known fact that the mean brightness of the glitter image as a function of the observation angle in the case of a narrow scatterometer diagram duplicates the distribution function of surface slopes.

Now we will proceed to a description of the properties of the signal in optical altimeters which are intended for measuring the distance between the surface and the instrument and which can be used in registering the large-scale (exceeding the dimensions of the resolution area) variations

APPROVED FOR RELEASE: 2007/02/08: CIA-RDP82-00850R000300010007-0

APPROVED FOR RELEASE: 2007/02/08: CIA-RDP82-00850R000300010007-0

of the surface level. The received signal in these instruments, the same as in scatterometers, is formed due to the reflection of the sounding field from surfaces with a mirror orientation relative to the altimeter. However, its statistical characteristics, in contrast to the signal for the scatterometer, are determined by the statistics not only of the slopes, but also the rises $\xi(r)$.

With the same assumptions as earlier, for altimeters operating at the nadir, it is possible to derive the following formula for a random realization of signal power at the photodetector input:

$$P(t, r_0)=\frac{a_u^2 R}{\pi\beta_u^2 h^2(a_u^2+a_u^2)}\iint_{-\infty}^{\infty} F\left(t-\frac{2(h(r_0)-\xi(r))}{c}\right)\times \exp\left\{-\frac{(r-r_0)^2}{\beta_0^2 h^2}-\frac{4(r_0-r+n_\perp h)^2}{a_u^2+a_u^2}\right\} dr, \quad (3)$$

where c is the speed of light; F(t) is a function describing the temporal change of the radiated power. For an altimeter operating with an SM beam $F(t) = P_0[1 + m \cos(\omega t + \varphi_0)]$, and for a pulsed altimeter describes the shape of the radiated pulse, and

$$\int_{-\infty}^{\infty} F(t)\,dt=w_0,$$

where w_0 is the total pulse energy.

We will assume that in an altimeter with an SM beam the information on the $h(r_0)$ value is obtained as a result of synchronous detection. [Signal heterodyning is more common, as was done, for example, in [7]. However, the use of any processing method is determined by the convenience of technical solutions and exerts no influence on the essence and final conclusions of the considered problem.] Then, if the wavelength of modulation is much greater than the wave height and variations of distance to the surface $\Delta h(r_0)$ and the phase of the reference signal is selected in such a way that the signal falls on the linear segment of the characteristic curve for the synchronous detector, at its output we obtain

$$A(r_0)=\frac{2KmP_0 a_u^2 \omega R}{\pi\beta_u^2 h^2(a_u^2+a_u^2)c}\iint_{-\infty}^{\infty} (\Delta h(r_0)-\xi(r))\times \exp\left\{-\frac{(r-r_0)^2}{\beta_0^2 h^2}-\frac{4(r_0-r+n_\perp h)^2}{a_u^2+a_u^2}\right\} dr, \quad (4)$$

where K is the coefficient of signal transformation in the photocathode-synchronous detector channel.

APPROVED FOR RELEASE: 2007/02/08: CIA-RDP82-00850R000300010007-0

APPROVED FOR RELEASE: 2007/02/08: CIA-RDP82-00850R000300010007-0

If it is also assumed that in a pulsed altimeter there is registry of a signal proportional to the relative lag time of the center of gravity of a received pulse, it is easy to demonstrate that its random realization is also described by expression (4). In this case the factor $Q_{SM} = mP_0\omega/c$ must be replaced by $Q_{source} = w_0 q/cT$, where q and T are parameters characterizing the processing unit; q is the steepness of the reference signal, T is the time constant of the integrator. The further results will be correct for both types of altimeters since the expressions for the random signal realizations in both cases coincide. It is useful to note that if the mean powers of the sources in these altimeters are identical, all other conditions being equal the accuracy of the measurements will also be identical, even with shot noise taken into account. [Some difference in the shot noise level can be associated with constant background illumination. When this is present pulsed altimeters have a greater accuracy than continuous altimeters.]

Averaging (4) for the set of surface realizations, we obtain the following expression for the mean signal:

$$\overline{A(\mathbf{r}_0)} = \frac{K a_{\text{и}}^2 \beta_{\text{и}}^2 Q_{\text{и.см}}}{4(\beta_{\text{и}}^2 + \beta_{\text{п}}^2) h^2 \sigma_\theta^2} \Delta h(\mathbf{r}_0). \tag{5}$$

[И = source; П = detector]

Thus, the value for the signal in the altimeter, averaged for surface realizations, is proportional to variations in the distance between the mean surface level and the altimeter.

In general, the formulas for the mean signal components are obvious and can be derived with less rigorous restrictions than those which were used in their derivation. However, these restrictions essentially simplify the computations when computing the second moments of the considered signals.

2. Energy Spectrum of Radar Signals

In evaluating the fluctuations we will proceed to a spectral description of the random processes (1), (4). We will assume that the characteristic spatial scale of the signal fluctuations in the scatterometer is much less than the characteristic scale of change of mean power. This assumption makes it possible to regard the process to be quasistationary (in space) and to compute the fluctuations by a standard method for some sector of the frame within which the observation conditions change to a negligible degree. In actuality this means that the $\varkappa_{0\perp}$ value in (1) can be considered constant and the spectral amplitude of the process (1) is represented in the form:

$$L(\mathbf{k}, \varkappa_{0\perp}) = \frac{1}{(2\pi)^2} \iint_{-\infty}^{\infty} P(\mathbf{r}_0, \varkappa_{0\perp}) e^{-i\mathbf{k}\mathbf{r}_0} d\mathbf{r}_0. \tag{6}$$

APPROVED FOR RELEASE: 2007/02/08: CIA-RDP82-00850R000300010007-0

APPROVED FOR RELEASE: 2007/02/08: CIA-RDP82-00850R000300010007-0

The energy spectrum G(k) of the random value $P(r_0, \varkappa_{0\perp})$ is related to the spectral amplitudes L by the expression [8]:

$$\overline{L(\mathbf{k}, \varkappa_{0\perp})L(\mathbf{k}', \varkappa_{0\perp})} = G(\mathbf{k}, \varkappa_{0\perp})\delta(\mathbf{k}-\mathbf{k}'). \tag{7}$$

Therefore, the procedure for computing the energy spectrum is reduced in essence to a determination of the spectral amplitude L of process (1) and computation of the $\overline{L(k)L(k')}$ value using the known two-point slope distribution function $w(n_\perp, n_\perp', \rho)$. As a result, for the energy spectrum of the signal in the scatterometer we obtain:

$$G_c(\mathbf{k}) = \frac{P_0^2 a_\pi^4 R^2}{(2\pi)^2 (2h\beta_\pi)^4} \int_{-\infty}^{\infty} \dots \int M(\mathbf{k}, \varkappa_{0\perp}, \mathbf{n}_\perp) M(\mathbf{k}, \varkappa_{0\perp}, \mathbf{n}_\perp') \times \tag{8}$$

$$\times w(\mathbf{n}_\perp, \mathbf{n}_\perp', \rho) e^{i\mathbf{k}\rho} d\rho d\mathbf{n}_\perp d\mathbf{n}_\perp',$$

where

$$M = \exp\left\{ \frac{[8h(\mathbf{n}_\perp - \varkappa_{0\perp}) - ik(a_\pi^2 + a_\pi^2)]^2 \beta_0^2 h^2}{4(a_\pi^2 + a_\pi^2)(a_\pi^2 + a_\pi^2 + 4\beta_0^2 h^2)} - \frac{4h^2(\mathbf{n}_\perp - \varkappa_{0\perp})^2}{a_\pi^2 + a_\pi^2} \right\}.$$

In order to evaluate the integral in (8) we will approximate the correlation function of surface rises in the following way:

$$B_\xi(\rho) = \begin{cases} \sigma_\xi^2 - \rho^2 \dfrac{\sigma_\theta^2}{2} & \text{with} \quad \rho \leqslant \rho_0 = \dfrac{2\sigma_\xi^2}{\sigma_\theta^2}, \\ 0 & \text{with} \quad \rho > \rho_0. \end{cases} \tag{9}$$

Then the function $w(n_\perp, n_\perp', \rho)$ assumes the form

$$w(\mathbf{n}_\perp, \mathbf{n}_\perp', \rho) = \frac{\exp\left\{ -\dfrac{n_\perp^2 + n_\perp'^2 - 2\Gamma(\rho)\mathbf{n}_\perp \mathbf{n}_\perp'}{2\sigma_\theta^2(1-\Gamma^2(\rho))} \right\}}{(2\pi)^4 \sigma_\theta^4 (1-\Gamma^2(\rho))}, \tag{10}$$

where

$$\Gamma(\rho) = \begin{cases} 1 & \text{with} \quad \rho \leqslant \rho_0, \\ 0 & \text{with} \quad \rho > \rho_0. \end{cases} \tag{11}$$

We introduce into (8) the factor $\exp(-\beta_0^2 z^2 k^2/2)$ corresponding to the averaging of the image over the area of the resolution spot on the ground. Then, substituting (10) into (8) and carrying out integration with (11) taken into account, we obtain the following expression for the energy spectrum of the signal in the scatterometer:

$$G_c(\mathbf{k}) = \frac{P_0^2 a_\pi^4 \beta_\pi^4 R^2}{64h^4(\beta_\pi^2 + \beta_\pi^2)^2 \sigma_\theta^4} \exp\left\{ -\frac{k^2 h^2 \beta_0^2}{2} - \frac{\varkappa_{0\perp}^2}{\sigma_\theta^2} \right\} \times \left[\frac{\sigma_\theta^2 S_0}{(2\pi)^2 \beta_0^2} + \delta(\mathbf{k}) \right], \tag{12}$$

APPROVED FOR RELEASE: 2007/02/08: CIA-RDP82-00850R000300010007-0

APPROVED FOR RELEASE: 2007/02/08: CIA-RDP82-00850R000300010007-0

where $S_0 = \pi\rho_0^2$ is the effective area of the correlation surface.

Expression (12) is correct if the S_0 value is much less than the area of the resolution spot ($\pi\beta_0^2h^2$). Precisely this inequality $\rho_0 \ll \beta_0 h$ makes it possible to use such a rough approximation of the correlation function as (9). As a result, we obtained the signal spectrum in the form of the sum of the spectrum of white noise passing through the filter, whose band is determined by the dimensions of the resolution spot and the discrete line at k = 0, describing the non-zero mean component of the process.

A similar evaluation of the energy spectrum is easily made for the signal in the altimeter. The procedure for computing the energy spectrum differs from that cited above only in that for averaging the product of spectral amplitudes it is necessary to use the joint two-point distribution function for rises and slopes. Omitting the intermediate calculations, we will cite a final expression for the energy spectrum of a signal in the altimeter. When $\Delta h(r_0) = 0$ the mean signal is equal to zero, the process is stationary and in accordance with (4), (6), (7) and (9) this expression has the form:

[И = source; пр = detector; СМ = SM]

$$G_a(k) = \frac{K^2 Q^2_{\text{и.см}} a_{\text{и}}^4 \beta_{\text{п}}^4 R^2}{16(\beta_{\text{и}}^2+\beta_{\text{п}}^2)h^4\sigma_\theta^4} e^{-\frac{k_{x_{\text{эк}}}^2}{2}} \frac{\sigma_\xi^2 S_0 \sigma_\theta^4}{(2\pi)^2\beta_0^4}. \qquad (13)$$

Thus, as in a scatterometer, the signal in the altimeter has the form of white noise passing through a filter whose parameters are determined by the directional diagram of the instrument.

3. Signal-to-Noise Ratio and Limiting Measurement Accuracy

Having expressions for the energy spectrum, it is easy to find the signal-to-noise ratio in the surface image. In instruments of the scatterometer type, in accordance with (12) this ratio is equal to:

$$\gamma = \sqrt{\frac{l_{\text{эк}}^2\beta_0^2}{2\rho_0^2\sigma_\theta^2}}, \qquad (14)$$

where $l_{el} = 2\beta_0 h$ is a linear resolution element on the surface. If the image is subjected to spatial filtering for the purpose of smoothing the spatial noise, in (14) it is necessary to replace $2\beta_0 h$ by the dimension of an element corresponding to the averaging window, which can be much greater than $2\beta_0 h$. However, it can be seen that the maximum signal-to-noise ratio is obtained in a case when the averaging occurs in image formation. This is associated with the circumstance that the γ value is proportional to the width of the scatterometer directional diagram and therefore the β_0 value must be the maximum admissible. We note that the integrand in (14) can be interpreted as the product of the number of independent (uncorrelated) surface sectors in a resolution element and the probability of the glitter falling in the scatterometer detector. In actuality, if we somewhat overdetermine the correlation radius of the

APPROVED FOR RELEASE: 2007/02/08: CIA-RDP82-00850R000300010007-0

APPROVED FOR RELEASE: 2007/02/08: CIA-RDP82-00850R000300010007-0

surface, then (14) can be represented in the following form:

$$\gamma=\sqrt{Np}, \tag{15}$$

where $p = \beta_0^2/2\sigma_\theta^2$, $N = l_{el}^2/\rho_0'^2$, $\rho_0' = \rho_0/2$. [The condition $\rho_0' = \rho_0/2$ corresponds to the following determination of the correlation radius: $\rho_0'^2 = \int B_\xi(\rho)\rho\,d\rho/B_\xi(0)$ with $B_\xi(\rho)$ described by formula (9).] Since formula (15) determines the number of gradations distinguishable in the received signal, the accuracy in measuring the dispersion of slopes in accordance with (2) (for the central part of the glitter image) is described by the expression:

$$\frac{\Delta\sigma_\theta^2}{\sigma_\theta^2}=\frac{\overline{\Delta P}}{\bar{P}}=\gamma^{-1}=\frac{1}{\sqrt{pN}}. \tag{16}$$

It should be noted that the derived expression (with $p \ll 1$) coincides with the known formula for the mean relative deviation of a process with a binomial distribution law [8]. Substituting into (15), (16) the explicit expressions for ρ_0 and l_{el}, we finally obtain:

$$\gamma^{-1}=\sigma_\xi/\beta_\theta^2 h. \tag{17}$$

It follows from (17) that the accuracy in measuring the dispersion of slopes is determined by only one surface parameter — mean square wave height. Expression (17) also determines the range of possible changes in instrument parameters -- the directional diagram and height. The choice of these parameters for a specific instrument is dependent on with what detail and accuracy, how rapidly and from what area it is necessary to collect information on the surface.

Similar reasoning is also possible for optical altimeters, although in this case the quantitative relationships between the accuracy in measuring height, state of the surface and instrument parameters will be different. It would be logical to expect that the accuracy in determining height is represented in the form of the product of the mean square height of waves σ_ξ and the value of the mean square error in measuring the dispersion of slopes described by formula (16). However, a comparison of formulas (5) and (13) leads to the following expression for the minimum detectable change in the distance between the altimeter and the mean surface level:

$$\Delta h_{min}=\frac{\sigma_\xi}{\sqrt{2}}\sqrt{\frac{1}{p^2N}}. \tag{18}$$

[MИH = min]

The difference between the anticipated evaluation for Δh_{min} and that derived on the basis of computations using formulas (5), (13) can be interpreted in the following way. If Δh_{min} is computed on the assumption of a statistical nondependence of the rises $\xi(r)$ and slopes $n_\perp(r)$, for Δh_{min}

APPROVED FOR RELEASE: 2007/02/08: CIA-RDP82-00850R000300010007-0

APPROVED FOR RELEASE: 2007/02/08: CIA-RDP82-00850R000300010007-0

it is possible to derive the formula

$$\Delta h_{\text{мин}} = \frac{\sigma_\xi}{\sqrt{2}} \sqrt{\frac{1}{pN}} = \frac{\sigma_\xi}{\sqrt{2}} \gamma^{-1},$$

[МИН = min]

which differs from the anticipated formula only by the factor $1/\sqrt{2}$. Therefore, the origin of the factor $1/\sqrt{2}$ is due to the finite correlation between the rise of the surface and its slope. As a result of this correlation in the signal registered by the altimeter the surface sectors corresponding to the wave crests and troughs are represented more frequently than the sectors situated near the mean level surface. In other words, the surface-altimeter system produces some effective filtering of the signals, leading to an increase in the scatter of the registered points. With respect to the origin of the factor $1/\sqrt{2}$, it is probably related to the finite dimensions of an independent surface sector participating in formation of the signal and corresponds to an effective averaging of its phase (height).

We will represent formula (18) in a different form:

$$\frac{\Delta h_{\text{мин}}}{\sigma_\xi} = \gamma^{-1} \frac{\sigma_\theta}{\beta_0}. \qquad (19)$$

[МИН = min]

Expression (19) shows that the relative accuracy of the altimeters (the error in determining distance, related to the mean square wave height) is always worse than the accuracy in determining the dispersion of slopes. This circumstance, as already noted, is related to the finite correlation between the slopes and rises.

An evaluation of the anticipated accuracy of scatterometers and altimeters in dependence on the surface state (wind velocity, units on the wave scale) and the requirements on the instrumentation without difficulty can be accomplished using formulas (16), (18) if we know the σ_ξ and σ_θ values, information on which can be found in studies [1, 2, 9-11]. When making specific computations it is only necessary to check satisfaction of the inequality $N \gg 1$ or $\rho_0^2 \ll \beta_0^2 h^2$. Otherwise formulas (16, 18) are incorrect.

In conclusion we will mention a number of obvious generalizations which the method developed in this study allows.

1. Although the final formulas were derived on the assumption of isotropicity of the waves, they also are correct in a general case. For anisotropic waves in formulas (14)-(16) it is necessary to make the replacement $\sigma_\theta = \sqrt{\sigma_{\theta x}\, \sigma_{\theta y}}$, where $\sigma_{\theta x}$, $\sigma_{\theta y}$ are the mean square slopes in two mutually perpendicular directions. With respect to the accuracy in

APPROVED FOR RELEASE: 2007/02/08: CIA-RDP82-00850R000300010007-0

APPROVED FOR RELEASE: 2007/02/08: CIA-RDP82-00850R000300010007-0

measuring $\sigma_{\theta_x}^2$ and $\sigma_{\theta_y}^2$, as before it will be determined by formula (17). It is easy to confirm this assertion if in place of (9) the correlation function of rises is approximated by part of an elliptical paraboloid.

2. This same evaluation is suitable for determining the accuracy in measuring the dispersion of slopes by scatterometers operating in a passive regime and registering the brightness distribution in the solar track. In this case, despite the fact that formulas (1), (2) and (12) are somewhat modified (primarily due to a different observation geometry), formula (16) retains its form for the central part of the image of the solar track.

3. The resulting accuracy evaluations can be regarded as limiting also for active radio scatterometers and radioaltimeters operating in the SHF range on the same principles as the optical instruments considered above. It goes without saying that they are incorrect in a case when the useful signal in these instruments is formed due to diffuse scattering and the glitter component is excluded due to an appropriate choice of the sounding angle. This case requires special investigation. This same comment also applies to optical altimeters registering the phase of radiation scattered in the near-surface water layer.

The author expresses appreciation to L. S. Dolin and Yu. M. Zhidko for a critical and useful discussion of the results in this study.

BIBLIOGRAPHY

1. Cox, C., Munk, W. H., "Statistics of the Sea Surface Derived from Sun Glitter," J. MARINE RES., 13, No 2, 198, 1954.

2. Cox, C., Munk, W. H., "The Measurements of the Roughness of the Sea Surface from Photographs of the Sun's Glitter," JOSA, 44, No 11, 838, 1954.

3. Muro, E. L., Pavlova, T. V., Fomin, N. S., "Experimental Determination of the Correlation Between Wind Direction and Velocity and the Height of Sea Waves With the Energy Characteristics of Light Pulses Reflected from the Sea Surface," TR. TsAO (Transactions of the Central Aerological Observatory), No 109, 101, 1975.

4. Mullamaa, Yu. A.-R., "Influence of the Wave-Covered Surface on the Visibility of Underwater Objects," IZV. AN SSSR, FAO (News of the USSR Academy of Sciences, Physics of the Atmosphere and Ocean), 11, No 2, 199, 1975.

5. Apel, J. R., "Ocean Science from Space," TRANS. AMER. GEOPHYS. UNION, 57, No 9, 612, 1976.

6. Soboleva, N. A., Berkovskiy, A. G., Chechik, N. O., Yeliseyev, R. G., FOTOELEKTRONNYYE PRIBORY (Photoelectronic Instruments), Moscow, "Nauka," 1965.

APPROVED FOR RELEASE: 2007/02/08: CIA-RDP82-00850R000300010007-0

APPROVED FOR RELEASE: 2007/02/08: CIA-RDP82-00850R000300010007-0

7. Olsen, W. S., Adams, R. M., "A Laser Profilometer," JGR, 75, No 12, 2185, 1970.

8. Rytov, S. M., VVEDENIYE V STATISTICHESKUYU RADIOFIZIKU (Introduction to Statistical Radio Physics), Moscow, "Nauka," 1966.

9. Kitaygorodskiy, S. A., FIZIKA VZAIMODEYSTVIYA ATMOSFERY I OKEANA (Physics of Interaction Between the Atmosphere and Ocean), Leningrad, Gidrometeoizdat, 1970.

10. VETER I VOLNY V OKEANAKH I MORYAKH. SPRAVOCHNYYE DANNYYE. REGISTR SSSR (Wind and Waves in the Oceans and Seas. Reference Data. USSR Register), Leningrad, "Transport," 1974.

11. VETROVYYE VOLNY (Wind Waves), edited by Yu. M. Krylov, Moscow, IL, 1962.

COPYRIGHT: Izdatel'stvo "Nauka," "Izvestiya AN SSSR, Fizika atmosfery i okeana," 1980

[269-5303]

5303
CSO: 1865

APPROVED FOR RELEASE: 2007/02/08: CIA-RDP82-00850R000300010007-0

APPROVED FOR RELEASE: 2007/02/08: CIA-RDP82-00850R000300010007-0

UDC 551.46.08

THEORY AND CALCULATION OF EQUILIBRIUM OF OCEANOGRAPHIC MEASURING SYSTEMS

Leningrad TEORIYA I RASCHET RAVNOVESIYA OKEANOGRAFICHESKIKH IZMERITEL'NYKH SISTEM in Russian 1979 signed to press 11 Oct 79

[Annotation, Preface and Table of Contents of book by N.F. Kudryavtsev]

[Text] A wide range of problems necessary for calculating a stable hydrodynamic equilibrium for arbitrarily loaded oceanographic measurement systems consisting of different types of towed or stationary measurement devices sequentially interconnected by a flexible, unstretchable cable is examined on the basis of well known results of modern mechanics and mathematics.

The monograph is intended for specialists occupied in the design and operation of oceanographic measurement systems and also for students of advanced classes of marine specialties.

This monograph is one of a number of studies which are highly specialized and it presents a consideration of an extremely important problem: the design of stationary and towed oceanographic measurement systems (buoy stations, series of bottom sampling water bottles and others) which, in the past 15-20 years literally revolutionized the technique and methods of marine research.

Nevertheless, reliable methods of designing the above mentioned systems did not exist previously, therefore the selection of parameters of their elements is not precise and error-free which, of course, greatly reduces the reliability, stability and, in the final analysis, the effectiveness of these methods of investigation.

Such a situation was complicated basically due to two fundamental difficulties. The first of these is connected with the selection of a law of hydrodynamic resistance of buoys, cables, situated on these devices and other elements of the systems and, second, is associated with previously

APPROVED FOR RELEASE: 2007/02/08: CIA-RDP82-00850R000300010007-0

APPROVED FOR RELEASE: 2007/02/08: CIA-RDP82-00850R000300010007-0

insurmountable difficulties. The author dealt with the first question by setting up special experiments in a hydrodynamic trough and obtaining the form of dependence of the drag on the angle of attack by an empirical method and he solved the second problem by means of numerical integration on an electronic computer.

As a result, the author was able to develop a method of calculation of all the basic elements of oceanographic measurement systems and also the loadings on them. The value of the results obtained for oceanographic (and not only oceanographic) observations, considering what was said above is difficult to overestimate.

TABLE OF CONTENTS

COPYRIGHT: Arkticheskiy i antarkticheskiy nauchno-issledovatel'skiy institut (AANII), 1979

[294-2791]
2791
CSO: 1865

APPROVED FOR RELEASE: 2007/02/08: CIA-RDP82-00850R000300010007-0

APPROVED FOR RELEASE: 2007/02/08: CIA-RDP82-00850R000300010007-0

UDC 528:061.3

PROBLEMS IN MARINE GEODESY

Moscow IZVESTIYA VYSSHIKH UCHEBNYKH ZAVEDENIY, GEODEZIYA I AEROFOTOS"YEMKA in Russian No 1, 1980 pp 115-119

[Article by Professor N. V. Yakovlev, Doctor of Technical Sciences, Moscow Order of Lenin Institute of Geodetic, Aerial Mapping and Cartographic Engineers]

[Text] The term "marine geodesy" was put into use for the first time in 1804 by the Russian researcher and navigator G. A. Sarychev. At that time the term was used to mean the complex of studies involved in hydrographic description of the seas (depth measurements), study of sea currents and the compilation of hydrographic charts.

The content of the term "marine geodesy" has now become incomparably broader and more complete. Marine geodesy is a branch of geodetic science and practice, the object of geodetic investigations being the world ocean, including the continental shelf.

At the present stage the principal scientific task of marine geodesy is the study and refinement of the parameters of the figure and gravitational field of the physical surface of the seas and oceans, coinciding or almost coinciding with the surface of the geoid, and also study of the topography and gravitational field of the bottom of the seas and oceans.

The principal scientific-technical task in marine geodesy essentially involves a determination, with geodetic accuracy, of the position of points or objects on the sea surface, on the bottom of the seas and oceans, and also within the water medium, and this in a unified coordinate system, as is particularly important, for example, in the system of the terrestrial ellipsoid.

These tasks are closely interrelated and are solved jointly. It must be noted that since ancient times the determination of the coordinates of sea ships on the surface of the seas and oceans has been the task of a special science -- marine navigation. However, the purpose and accuracy of these determinations in this case are somewhat different than in marine geodesy. The task of marine navigation includes ensurance of safe

APPROVED FOR RELEASE: 2007/02/08: CIA-RDP82-00850R000300010007-0

APPROVED FOR RELEASE: 2007/02/08: CIA-RDP82-00850R000300010007-0

navigation. Until the recent past in marine navigation there has been no need for the exceptionally high accuracy in determining coordinates which is characteristic of geodetic measurements in the study of great expanses of the earth's surface and the world ocean in topographic-geodetic and gravimetric respects.

In determinations of the position coordinates of ships in the world ocean both for navigational purposes and for the purposes of marine geodesy, at the present time extensive use is made of satellite, radionavigation, on-board inertial and other systems, more and more frequently being combined into so-called integral systems or automated measurement complexes for the purpose of increasing the accuracy in determining coordinates.

The accuracy of all these measurement systems from the point of view of solution of scientific and practical problems in marine geodesy for the time being is still inadequate. Accordingly, the problem arises of further improvement and development of a new measuring system with an accuracy not less than an order of magnitude greater, which can be employed for determining the coordinates of points on the surface of the seas and oceans. This involves solving a great number of diverse problems and tasks associated with the development and creation of more precise instrumentation, the development of more modern determination theories and methods and allowance for the influence exerted on the measurement results by a variety of sources of errors, including instrument errors and the environment. The problem also arises of developing and improving algorithms for the mathematical processing of measurement results.

Satellite altimetry has successfully been introduced for studying the topography of the sea surface. The next task is to reach reliably the 10-cm level of accuracy in measuring the relative rises of the sea surface with a simultaneously high accuracy in determining the orbital elements and positions of artificial earth satellites in orbit during each observation period. It is necessary to carry out a considerable volume of scientific research and experimental-practical work so that it will be possible to detect not only large, but also small waves of the geoid reliably and with a high accuracy and ascertain the height of the geoid above the terrestrial ellipsoid with errors not greater than one or two meters at any place in the world ocean.

As indicated by the results of satellite altimetry, the physical surface of the seas and oceans, under the influence of the wind, tidal phenomena, changes in air pressure and other factors, does not coincide with the surface of the geoid; it constantly changes its vertical position relative to the geoid and the sea floor, sometimes up to 10 m. Failure to take this circumstance into account invariably leads to the appearance of errors in computing corrections for reduction of the measurement results to the surface of the terrestrial ellipsoid. For example, with deviation of sea level by only 5 m from the surface of the geoid a failure to take this deviation into account causes an error of about 1.5 mgal with reduction of gravity to the terrestrial ellipsoid, inadmissible in precise measurements.

APPROVED FOR RELEASE: 2007/02/08: CIA-RDP82-00850R000300010007-0

APPROVED FOR RELEASE: 2007/02/08: CIA-RDP82-00850R000300010007-0

Attention must also be given to the fact that registry of the deviations of sea level (vertically) from the surface of the geoid must be accomplished synchronously with gravimetric and geodetic measurements made aboard a ship. There is still no answer as to how to solve this problem. In this case satellite altimetry may be useless because at each moment in time when gravimetric and geodetic measurements are being made the satellite altimeter as a rule will not fly over the vessel but possibly hundreds and thousands of kilometers from it. The following problem arises: how, by what means and by what methods at each moment of geodetic and gravimetric measurements is it possible to determine the vertical deviations of sea level from the surface of the geoid so that with a suitable accuracy it will be possible to reduce the measurement results to the surface of relativity?

The following work must be done in connection with the multisided study and mastery of the world ocean and coastal shelf:
-- mapping of the sea bottom at different, including large scales;
-- implementation of different kinds of engineering-technical work on the sea floor, related, in particular, to exploration for petroleum and gas and its production, working of mineral resources, laying and repair of pipelines, cables, etc.;
-- study of tides and sea currents;
-- determination of sea surface slopes;
-- study of the life in abyssal depressions and large underwater ridges in the world ocean, etc.

In order to carry out these and a great many other types of work, to be accomplished at sea, it is necessary that a geodetic control network be created on the sea floor, this being a continuation of the continental geodetic network and using the same system of coordinates and elevations; this network must be constructed with the highest possible degree of accuracy.

In principle there must be a geodetic control network over the entire area of the world ocean. However, for the immediate foreseeable future a solution of this problem is not within the capabilities of any one country due to technical and economic considerations. Accordingly, bottom networks of primarily local significance will for the most part be created. However, individual bottom stations can and evidently will be established in different regions of the world ocean.

The creation of a geodetic network of control points both on the land and on the sea floor begins with the development of the scientific and technical conditions which this network must satisfy. Applicable to the conditions of the seas and oceans such scientific and technical requirements have yet to be satisfied. In the not too distant future this rather complex problem will be given priority and it will be necessary to discuss it in all details, taking into account a variety of needs of different departments interested in the creation of a geodetic control network on the floor of the seas and oceans.

APPROVED FOR RELEASE: 2007/02/08: CIA-RDP82-00850R000300010007-0

APPROVED FOR RELEASE: 2007/02/08: CIA-RDP82-00850R000300010007-0

Next the problem arises of choosing the most desirable scheme and program for constructing this network. This problem must be solved taking into account the specifics of fixation of the stations on the sea floor and determination of their coordinates.

It is understandable that bottom geodetic stations in the seas and oceans in their design have nothing in common with triangulation and polygonometric stations. Sea control stations are passive or active hydroacoustic transmitters. The development and creation of hydroacoustic bottom stations, optimum in a definite sense, is a rather complex scientific and technical problem. A number of designs of acoustic systems have now been developed for the fixation of bottom stations, but they all require further improvement for the purposes of increasing the range and duration of their effect, and also increasing their economy.

The determination of coordinates of stations in the geodetic network on the sea floor with an accuracy even two orders of magnitude less than in the modern first- - fourth-order geodetic networks created on the land is an exceedingly difficult problem. The reasons for this circumstance rest in the complexity of the transfer of coordinates from the earth's surface to the sea floor. These difficulties increase appreciably with increasing distance of sea stations from the stations in the continental geodetic network with known coordinates and also with an increase in depth of the sea bottom.

In a general case the transfer of coordinates to stations in the geodetic control network created on the sea floor is accomplished using the following approximate scheme: at the time of observation an automated measurement complex is employed in ascertaining the instantaneous coordinates of the vessel on the sea surface and from that moment -- the track of the ship. Simultaneously with these observations, using hydroacoustic systems, measurements of slant distances are made from specific points on the vessel to bottom stations in accordance with some scheme most desirable under specific circumstances. All these measurements are made at a real time scale.

By knowing the coordinates of the ship and the distances between the ship and the station to be determined on the sea floor at some moments in time it is easy to compute the coordinates of this station from solution of repeated linear intersection. There can also be other variants of solution of the particular problem, but the basic principle in step-by-step determination of the coordinates first of the surface ship at some moments in time and then through it, the coordinates of the station on the sea bottom, is retained. In order to increase the accuracy in constructing a bottom network it is necessary to make additional measurements of the distance between its adjacent points, for example, by the method of intersection of the acoustic line between them and then adjustment of the network for all the geometric conditions arising in it.

APPROVED FOR RELEASE: 2007/02/08: CIA-RDP82-00850R000300010007-0

APPROVED FOR RELEASE: 2007/02/08: CIA-RDP82-00850R000300010007-0

At the present time the accuracy in determining the coordinates of stations on the sea bottom is still inadequate from the geodetic point of view, especially in the case of a considerable distance of these points from the shore line and great depths of the seas and oceans. An exceedingly difficult problem is bringing about a substantial increase in the accuracy in determining the coordinates of bottom stations in the world ocean. In this connection it is necessary to solve a wide range of highly complex scientific and technical problems and tasks. We will note some of them.

It is necessary to increase the accuracy in determining the position of the vessel on the sea surface by one or two orders of magnitude, especially at the times of observations, and also the accuracy in reckoning the ship's track between observations; there must be a substantial increase in the accuracy of hydroacoustic measurements of distances and directions between bottom stations and acoustic detectors installed aboard a ship. There is a need for a more detailed and precise study of the figure and gravitational field of the surface of the geoid in the seas and oceans; it is necessary to develop means and methods for determining changes in the height of the sea surface and the ship relative to the surface of the geoid or the sea bottom during the period of observations and reckoning of the ship's track.

Despite the complexity and great cost of modern measurement complexes installed aboard scientific research ships, they nevertheless do not ensure the required high accuracy in geodetic determinations of the instantaneous coordinates of a vessel on the sea surface. In this connection much research work is planned on the further improvement and substantial increase in the instrumental accuracy of automated measurement complexes and the development of the most effective methods for discriminating and taking into account the systematic errors in the results of measurements made using this apparatus.

In solving the latter problem it is necessary, in particular, to create special sea standard polygons intended for the calibration of sea measurement complexes. It is desirable that polygons be established in the most characteristic regions of the seas and oceans. Such polygons will make it possible not only to carry out calibration of sea measurement systems and complexes, but also to carry out a wide range of scientific investigations for the purpose of developing the most effective means and methods for sea measurements of different kinds -- geodetic, gravimetric, etc.

A broad range of complex problems arise in connection with the need for a substantial increase in the accuracy of hydroacoustic measurements of distances when creating bottom geodetic networks, and in particular, the problem of determining the most precise velocity of sound propagation along each specific line in the sea medium at the time when these measurements are made.

APPROVED FOR RELEASE: 2007/02/08: CIA-RDP82-00850R000300010007-0

APPROVED FOR RELEASE: 2007/02/08: CIA-RDP82-00850R000300010007-0

We note in conclusion that the principal, fundamental problems and tasks in marine geodesy for the most part remain the same as in geodesy as a whole. The principal and fundamental differences essentially involve the development and use of other means and methods for all types of geodetic, gravimetric and other types of work in the seas and oceans caused by the specifics of marine conditions.

The sharp difference between the water medium and the earth's solid crust on the land, the temporal and spatial variability of the surface of the seas and oceans, the poor transparency of the water medium in comparison with atmospheric transparency, the absence of any possibility for visual inspection of the surface of the sea floor, etc., all these factors taken together place before geodetic science and practice a number of highly complex problems and tasks which geodesists earlier virtually never have had to deal with and which now must be solved.

In order to carry out geodetic and gravimetric studies at sea it is necessary to have not only specific methods and measurement apparatus, but most of all specialists who have mastered the complex measurement techniques and methods and who are capable of implementing this work under the difficult conditions at sea with high quality and at a high scientific level.

Taking this circumstance into account, specialists at the Moscow Institute of Geodetic, Aerial Mapping and Cartographic Engineers have begun the planned training of astrogeodesists for work at sea. Since 1974, on the initiative of the Institute's Rector, V. D. Bol'shakov, there has been a field of specialization in the fourth and fifth years of the astrogeodesy curriculum and each year there are instructional-practice and practical field work sessions for a group of students in the third and fourth years of the Department of Higher Geodesy. In these sessions the students and instructors acquire the necessary work experience at sea on the geodetic support for marine geological-geophysical surveys on the continental shelf of the country.

COPYRIGHT: Geodeziya i aerofotos"yemka, 1980

[329-5303]

5303
CSO: 1865

APPROVED FOR RELEASE: 2007/02/08: CIA-RDP82-00850R000300010007-0

APPROVED FOR RELEASE: 2007/02/08: CIA-RDP82-00850R000300010007-0

OPTIC METHODS OF STUDYING OCEANS AND INTERNAL RESERVOIRS

Novosibirsk OPTICHESKIYE METODY IZUCHENIYA OKEANOV I VNUTRENNIKH VODOYEMOV (Optic Methods of Studying Oceans and Internal Reservoirs) in Russian 1979 signed to press 16 Mar 79 p 2, 354-357

[Annotation and table of contents from book edited by Grigoriy Ivanovich Galaziy and Kusiel' Solomonvich Shifrin, Nauka, 1,450 copies, 359 pages]

[Text] This book examines the use of optic methods in the visible and infrared ranges to study oceans and internal reservoirs. The collection has been prepared from materials of the third plenary session of the ocean optics branch in the Oceanographic Commission of the USSR Academy of Sciences, and consists of the following sections: general questions on long-range measurements and the optics of reservoirs; study of the color and spectrum of the outgoing light to evaluate the chlorophyll and suspended matter in the water; optic methods of studying wave action; long-range methods of measuring pollution; study of surface radiation temperature; problems of optics of lakes and land water in relation to long-range investigation methods; the light field in reservoirs and long-range measurement methods.

The collection is designed for scientific workers, engineers, post-graduate students and students that are interested in questions of environmental protection, physical oceanology and limnology, and long-range measurement methods.

Contents

APPROVED FOR RELEASE: 2007/02/08: CIA-RDP82-00850R000300010007-0

APPROVED FOR RELEASE: 2007/02/08: CIA-RDP82-00850R000300010007-0

*Asterisk marks works presented as summaries.

APPROVED FOR RELEASE: 2007/02/08: CIA-RDP82-00850R000300010007-0

APPROVED FOR RELEASE: 2007/02/08: CIA-RDP82-00850R000300010007-0

APPROVED FOR RELEASE: 2007/02/08: CIA-RDP82-00850R000300010007-0

APPROVED FOR RELEASE: 2007/02/08: CIA-RDP82-00850R000300010007-0

APPROVED FOR RELEASE: 2007/02/08: CIA-RDP82-00850R000300010007-0

APPROVED FOR RELEASE: 2007/02/08: CIA-RDP82-00850R000300010007-0

COPYRIGHT: Izdatel'stvo "Nauka," 1979

[336-9035]

9035
CSO: 1865

APPROVED FOR RELEASE: 2007/02/08: CIA-RDP82-00850R000300010007-0

APPROVED FOR RELEASE: 2007/02/08: CIA-RDP82-00850R000300010007-0

TERRESTRIAL GEOPHYSICS

HOLOGRAPHY AND OPTICAL DATA PROCESSING IN GEOLOGY AND GEOPHYSICS

Leningrad GOLOGRAFIYA I OPTICHESKAYA OBRABOTKA INFORMATSII V GEOLOGII I GEOFIZIKE in Russian 1979, pp 2-4, 193-194

[Annotation, table of contents and introduction from book edited by S. B. Gurevich, Order of Lenin Physico-Technical Institute imeni A. F. Ioffe, Leningrad, 500 copies, 195 pages]

[Text] Annotation

Reports read at the All-Union Seminar on Optico-electronic Methods of Processing Geological and Geophysical Data, held in Tomsk in 1978, served as the basis for the present collection. The main theme of the collection is the processing of large masses of geophysical data and the creation of new instruments and devices for the optical processing of geological and geophysical materials. Specific methods and devices are examined along with survey reports on that theme. The materials presented in the articles are of great importance for the development of work envisaged by the national economic plan. They provide the possibility for specialists, geophysicists and geologists to become acquainted with the new possibilities opened up by holography and methods of optical data processing in tasks of searching and prospecting for minerals.

CONTENTS

APPROVED FOR RELEASE: 2007/02/08: CIA-RDP82-00850R000300010007-0

APPROVED FOR RELEASE: 2007/02/08: CIA-RDP82-00850R000300010007-0

APPROVED FOR RELEASE: 2007/02/08: CIA-RDP82-00850R000300010007-0

APPROVED FOR RELEASE: 2007/02/08: CIA-RDP82-00850R000300010007-0

Introduction

The complexity of the problems to be solved in the search for petroleum, gas and solid mineral resources requires a considerable increase of computer capacities and the development of methods and means of effective processing of geological and geophysical data. Computer compleses based on second and third generation electronic computers existing at the present time do not completely meet contemporary requirements, in connection with which a number of important and necessary algorithms for the processing of geological and geophysical data often are not realized in practice. It should be expected that in proportion to the development of work on area systems of observations and seismic holography the requirements for the efficiency and operativeness of data processing will grow still more. In that respect much interest is aroused by the further improvement of digital means of data processing as well as the development of optical and optico-electronic methods which have considerable possibilities with respect to the processing and storage of large flows of data.

At the present time in a number of scientific and production organizations and VUZ's of the country experience has been accumulated in the development and use of optical computer systems, experience that confirms the prospects of development of that direction of automation of the processing of data of exploration geophysics and geology.

The First All-Union seminar on the optico-electronic processing of geological and geophysical data, held in 1978 in Tomsk, summed up definite results of investigations in that area.

The present collection contains reports read at the seminar that were devoted to questions in the development and investigation of optical computing devices and hybrid optico-electronic data processing systems. Some methodical and technological methods of processing, directed toward improvement of the methods and means of processing geological and geophysical materials, are examined.

The publication of the collection, in our view, will undoubtedly have a positive influence on the further conducting of investigations and will permit acquainting specialists with the results achieved in this area.

APPROVED FOR RELEASE: 2007/02/08: CIA-RDP82-00850R000300010007-0

APPROVED FOR RELEASE: 2007/02/08: CIA-RDP82-00850R000300010007-0

It is proposed to continue in the future the discussion of optico-electronic methods and means of processing geological and geophysical data and to issue subsequent collections of articles.

Professor S. B. Gurevich and candidates of technical sciences V. P. Ivanchenkov and O. A. Potapov

COPYRIGHT: LIYaF, 1979
[291-2174]

2174
CSO: 1863

- END -

APPROVED FOR RELEASE: 2007/02/08: CIA-RDP82-00850R000300010007-0